May 2018

Impact Load Identification Using Optimal Sensor Placement and Model Reduction

Bella Jackson Chembakassery
University of Wisconsin-Milwaukee

IMPACT LOAD IDENTIFICATION USING OPTIMAL SENSOR PLACEMENT AND MODEL REDUCTION

by

Bella J Chembakassery

A Thesis Submitted in

Partial Fulfillment of the

Requirements for the Degree of

Master of Science

in Engineering

at

The University of Wisconsin-Milwaukee

May 2018

ABSTRACT

IMPACT LOAD IDENTIFICATION USING OPTIMAL SENSOR PLACEMENT AND MODEL REDUCTION

by

Bella J Chembakassery

The University of Wisconsin-Milwaukee, 2018
Under the Supervision of Professor Anoop K. Dhingra

Any structure which is used in service can be subjected to different kinds of loads such as static, dynamic, moving or impact loads. It is very much necessary such structures are reliable and robust enough to be used for service. Hence accurately estimating the load acting on the structure is very important. In case of impact loading, it is very difficult to estimate the load because it acts for a short period of time. For such loading, the structural response of the system can be used as a medium to estimate the applied load. The structural response used could be strain or displacement. This is known as the "inverse problem".

The response cannot be measured at the locations on the structure as this will be cost-prohibitive. The inverse problem techniques encounter some limitations such as usage of limited number of sensors due to financial constraints, inaccessible location to place the sensor and the influence of sensor on the structural response. Due to these limitations, it is very much obvious that the load estimates have few errors. By choosing the correct optimum locations to place the sensors, it is possible to minimize these errors.

The impact load is recovered in this work by using the strain values at the chosen optimum locations. The technique used to choose the optimum location to place the sensors is called D-optimal technique. In this thesis, the D-optimal technique is used extensively. The recovery of impact loads through measurement of structural response at a

finite number of optimally selected location is demonstrated. This optimum sensor locations are identified using the D-optimal design Algorithm. Separate algorithms are developed to recover the impact load. ANSYS APDL 17.2 and MATLAB are programming software were used to estimate the applied loads. Based on the results obtained from several numerical examples, it is seen that the technique presented gave fairly accurate load estimates.

Dedicated to my grandparents *K.V. Paul* and *Lilly Paul*,
for their unconditional love, support and motivation.

TABLE OF CONTENTS

LIST OF FIGURES

LIST OF TABLES

ACKNOWLEDGEMENTS

First and foremost, I would like to express my deepest gratitude to my advisor Dr. Anoop K. Dhingra for providing me an excellent opportunity to do research under his guidance. His valuable guidance and support during my enrollment as a student at University of Wisconsin - Milwaukee is the main reason behind the success of this thesis.

I am grateful to my thesis committee members Dr. Nathan Salowitz and Dr. Nidal Abu-Zahra for investing their valuable time to go through my work and for their insightful comments and suggestions.

I express my profound sense of gratitude to Paul Augustine, for his valuable and continuous support in completing this thesis work. I would like to thank Kedar A Malusare, Project Engineer, FE Analyst at Stutzki Engineering for his valuable inputs. Special thanks to my friend Priyanka Pillai, Supplier Quality Engineer at Broan and Nutone who was a great support throughout my Master's Program at University Of Wisconsin, Milwaukee. I would also like to thank Brian Hansen, Vice President of Business Process Management at Switchgear Power Systems LLC, and my colleagues at Switchgear Power Systems LLC, for their patience and encouragement which played an important role in completion of my thesis.

My sincere thanks goes to my lab colleagues Hana Alqam, Bibek Wagle and Hussain Altammar for their invaluable inputs and suggestions.

Above all, words cannot express how grateful I am to my parents who raised me with a love for science and supported me in all my pursuits, and for their unconditional love and care. Special thanks to my brother Sohan who was a great influence during my engineering program and my cousins for their love and motivation. Last but not least, I would like to thank my grandparents for their support, encouragement and great patience during the various stages of this thesis. I know I always have my family to count on when times are rough. I would not have made it this far without them.

1 Introduction

1.1 Problem Statement

A load which acts on a structure for a short duration of time is called as impact load. Whenever an impact load is imposed on a structure, there is an abrupt exchange or absorption of energy, which can cause a lot of vibration and drastic changes in velocity. Stresses caused by colliding members may be several times larger than the stresses produced by the same loads applied statically (when they are at rest). The vibrations caused by the impact load can severely damage the structure. Hence it is very much necessary to have the information of the exact value of the load while designing the structure. The method of identifying the exact value of an impact load is called as impact load identification. By knowing the exact value and location of the load, it is possible to have a cost effective design for the structure and as well as reduce any damage to the structure.

1.2 Limitations Of Load Cells

Generally, load cells are placed between the structure and the load causing body to determine the applied load. These load cells then measure the load acting on the structure by the body. This direct measurement of load by load cells is not applicable for some cases. The few limitations of load cells are as follows:

1. Load cells may affect the dynamic characteristics of the system, which may differ from the original system.

2. It is difficult to place load cells for certain types of loads applied on the structures such as wind loads, seismic excitation, aerodynamic loads etc.

3. Inaccessibility of the location where the load is applied may not allow the user to place the load cell at the desired location.

4. The load has to be directly in contact with the load cell for the measurement, hence making the direct measurement method less flexible.

1.3 Using Structure as a Load Cell

It is easier to measure the response such as strains, displacements, velocities, accelerations etc of the structure to find the unknown applied load. This implies that if structure acts like a load cell, the measurement of the loads can be done by the sensors placed on the structure. This indirect method is more reliable than the direct method, since this method overcomes all the limitations of the direct method.

1.4 Limitations of Inverse Load Identification Method

Inverse problems generally are very ill-conditioned. If the matrices are ill-conditioned it is difficult to solve the linear equations, which can give inaccurate results. This ill-conditioning happens because it is not possible to measure the response at all locations. The locations are randomly selected where the sensors are placed and the response is measured. The number of sensors used are limited to make the procedure cost-effective. More number of sensors can affect the system response. Sometimes some points are inaccessible for placing the sensor. Due to these drawbacks the important response information will not be taken into consideration which may result into inaccurate results. For impact load, the ill-condition is also caused due to the noise in measurements. Various techniques have been used in past to solve these drawbacks, these techniques are briefly explained in Chapter 2.

1.5 Organization of the Material

Chapter 1 gives a brief explanation of the impact load estimation problem. It gives an overview of the thesis and answers various questions. Also it discusses the challenges

involved during the course of this thesis.

Chapter 2 presents a literature review which gives detailed summary of the methods, algorithms and the works of previous authors who worked in the field of impact load identification. There are pros and cons for the algorithms discussed in this chapter and the need for a new algorithm is clearly explained.

Chapter 3 explains the algorithm used to recover the impact load where strain value is used as the response. Before applying this algorithm to recover the impact load, this method was applied to quasi-static, bent cantilever beam numerical example and results were obtained. In the similar way, the results for impact load were obtained and are discussed.

Chapter 4 uses a different technique for impact load recovery where strain value was the measured response. The algorithms from chapter 3 are used extensively. Chapter 4 deals with model reduction which is the most important chapter in this thesis. This concept of model reduction was used on a discrete as well as on a continuous system.

Chapters 5 and 6 present major findings of this thesis and also the scope for future work. Some potential areas of future work are discussed based on the results obtained in the earlier chapters.

2 Literature review

In the aerospace industry, impact load location and recovery has been an important area of research. The impact loads can cause a lot of change to the material as well as can do a lot of damage. If the impact load is not predicted accurately, it can cause fatal accidents. Several techniques have been developed to identify the impact load location and recover the load. Most of these techniques include measuring the structural responses such as strain, displacement, acceleration, and bending moment, to predict the applied load. There are few factors which effect the accuracy of obtained results such as the algorithm used for the experiment, including static and dynamic properties of structure and location of the sensors placed on the structure. Some of the techniques used in the past to recover impact loads are discussed in this chapter.

2.1 Impact Load Identification

Theoretical methods have been developed by many researchers to recover impact load. *Hillary and Ewins (1984)* tested a cantilever beam by using two sinusoidal loads with same frequency but different magnitude, but the results were poor and ill-conditioned. *Desanghere and Snoeys (1985)* conducted experiments on a real longitudinal beam of a car frame excited by three electromagnetic shakers, and researched extensively influences on the identification of results, such as noise on dynamic responses, perturbation of modal parameters and limited number of modes from an analytical example by the Modal Coordinate Transformation Method(MCTM). But this method was weak due to the lack of structural modes participating.

A recent research by *A.Alipour and F.Zareian,(2008)* force is calculated assuming Rayleigh damping *Rayleigh, (1954).* Here a Multi-Degree of Freedom (MDOF) is used:

$$M\ddot{x}(t) + C\dot{x}(t) + Kx(t) = F(t) \tag{2.1}$$

Usually to solve these equation, the Mass [M], Stiffness [K] matrices are assumed to be known. Here the damping matrix can be defined as a function of mass and stiffness matrices. The damping ratio of such system is given as:

$$\zeta_i = \frac{\alpha}{2}\frac{1}{\omega_i} + \frac{\beta}{2}\omega_i \tag{2.2}$$

Damping ratios can be calculated using the Caughey series *Caughey and OKelly,(1965)*, Rayleigh damping is a special case known as proportional damping or classical damping model which expresses damping as a linear combination of the mass and stiffness matrices, that is,

$$C(t) = \alpha M(t) + \beta K(t) \tag{2.3}$$

where [C] is damping matrix. The value for mass, stiffness and damping matrices are substituted in equation(2.1) to find the force.

Medina and Krawinkler (2004) proposed modeling each beam element with a combination of an elastic beam element and rotational end springs. Plastic hinging occurs in these zero length rotational spring elements with zero damping. As the initial stiffness of the spring is set to be large, all the elastic deformations occur in the beam with the given damping. This will result in stiffness proportional damping which will be relevant to the stiffness of the elastic beam and eliminates the effect of ambiguous forces resulted from stiffness proportional part of the damping in nonlinear cases.

Zareian (2006) proposed an extension to the solution proposed by *Medina and Krawinkler (2004)* for proper modeling of viscous damping using the Rayleigh model that can be applied to beam or column elements whose moment gradient can vary with time. This extension is useful in modeling beams and columns in Multi-Degree-Of-Freedom (MDOF) systems. Zareian's solution involves changing the stiffness matrix of the elastic internal beam element explained previously such that the effect of fixed stiffness of the

springs at the two ends of the elastic beam element is compensated.

2.2 Techniques used to Recover Impact Load

Many techniques were used to detect the location for impact load as well as recover the load. *Huang and Pan (1997)* used inverse techniques for the prediction of impact forces from acceleration measurements on a vibratory mill. A method based on optimization approach has been developed to predict the impact force by minimizing the difference between the measured acceleration and the predicted acceleration from the solution of the modal equations. *Khoo and Ismail (2013)* used the methodology of Operating Deflection Shape (ODS) analysis, Frequency Response Function(FRF) and pseudo-inverse to evaluate the impact load. A rectangular plate was used as test rig, where the good and bad locations for the sensors were based on the condition number. The impact load was calculated for three cases: under-determined, even determined and over-determined cases. The results were reliable for even determined and over-determined but under-determined gives inaccurate results. *Yang and Zhou (2009)* used genetic algorithm to reconstruct impact load on composite structure at impact location. A similar method by *Ajmari and Yang (2013)* determined the impact location and impact load by triangulation method and the impact location was further refined by minimization of an objective function through particle swarm optimization method(PSO). *Rajbhandari (2016)* developed a method to detect impact load location using Time Difference of Arrival (TDOA) where the difference in arrival times of the signals at each receiver is estimated. The intersection of the hyperbolas will give a finite impact load location.

2.3 Optimum Sensor Location

Many techniques have been developed over the years to solve the inverse problem. Most of the techniques used so far were ill-conditioned systems. With the help various methodologies, most of the ill-conditioning has been avoided. A study by *Stevens(1987)*

explains excellent techniques to solve such inverse problems. A technique of converting the inverse problem to minimization problem was proposed by *Busby and Trujillo (1986)*. This minimized the difference between the predicted structural response and measured structural response. A statistical analysis was conducted by *Masroor and Zachary (1991)*, where they recovered the load using strain measurement at a certain number of locations. Their study was the most significant as the recovered load turned out to be very accurate. They have explained that it is very much necessary to know the feasible location for the sensors for accurate load recovery. Their study showed that the variance of the load estimates were directly related to the sensor location. In their study it is expected the user should select these optimum location manually. But there were chances that these locations could possibly not be feasible and may give inaccurate results.

Further development was made to this technique by *Gupta (2013)*. In his study the optimum strain location is identified using D-optimal technique (determinant-optimal) which utilizes the k-exchange algorithm to select optimum sensor locations. This D-optimal used in *Gupta(2013)* study was developed by*Mitchell (1974)*, *Galil (1980)* and *Johnson et al (1983)*. This algorithm only selects the best sensor location from the available locations. D-optimal design method is also used in this thesis to identify the optimum strain gage orientation.

2.4 Summary

The best example for an inverse problem is a an indirect load identification problem. The smallest error in measurement can result in inaccurate results. Therefore, problem conditioning must be improved through optimal placement of sensors. Any dynamic problem with distributed, moving and impact load are all inverse load problems. The inverse method to identify load clearly lacks the identification of correct location for the placement of sensors. As explained above, some of the researchers had a prior knowledge of the optimum location which led to accurate results. But in real life, the location have to be

estimated. In this thesis, the solution for the sensor placement problem is discussed.

3 Recovery of Quasi-Static and Impact Loads Using Strain Measurements

Load recovery using inverse analysis has been used for several years. The strain values are measured at certain location using strain gages. In this chapter, a new method is used to recover quasi-static and impact loads. The key procedure in this thesis is to identify the optimum location of the strain gages and estimate the applied loads which is explained in Sections 3.1 to 3.4

3.1 Theoretical Development

There is a linear relationship between the force and strain response of a linear structure. Equation(3.1) has been developed for a structure when quasi-static load is applied. This equation is written as:

$$[\varepsilon(t)] = [A][F(t)] \tag{3.1}$$

where $\varepsilon(t) \subset R^{m \times t}$, m are strain gage locations, t is the number of time steps, [A] is the system matrix and [F(t)] is the applied load. [F(t)] $\subset R^{n \times t}$ where n are applied loads at t time steps.

The load can be calculated inversely by using a method called as the left-pseudo inverse method of least square estimates. Here the values of the system matrix and the measured strain values are assumed to be known. Equation(3.2) shows the calculation of imposed load:

$$[F(t)] = ([A]^T[A])^{-1}[A]^T[\varepsilon(t)] \tag{3.2}$$

where [F(t)] is the recovered load and $[\varepsilon(t)]$ are the strain values which were already measured. The accuracy of the estimation can be determined by using the variance of the

estimated load. In this case it is assumed that the variance-covariance matrix for load estimates are distributed independently which can be calculated by the equation given as follows:

$$var(F) = \sigma^2([A^T A])^{-1} \tag{3.3}$$

where σ and σ^2 is the standard deviation and variance of strain measurements respectively. $[A^T A]^{-1}$ is the sensitivity matrix of [A]. The smaller is the value of the sensitivity matrix, more precise will be the load recovery. On this notion, the entire D-optimal design algorithm is built. The minimum sensitivity matrix is formed by optimum set of strain gages, the angular orientation of strain gages and the location of the strain gages. To get the minimum value of sensitivity of [A], a computational technique is used so that the optimum combination as mentioned before can be obtained. The sensitivity of [A] can be reduced if the determinant of its sensitivity matrix $[A^T A]$ is maximized.

The load when applied to a certain node will affect the entire system. For all the numerical experiments conducted the strain data is only obtained at the optimum locations. The load history only recovered at the place where the load is applied. This technique will be used to recover the impact load which is explained in the next section. By using interpolation technique it is possible recover the load history. As mentioned earlier the load is only recovered at the point where it applied, but is possible to estimate the load at other locations too using the interpolation technique. For static and quasi-static load cases, linear interpolation will be sufficient but for dynamic impact loads, higher-order interpolation techniques will have to be used. For such cases, there is interpolation function called as 'SPLINE' in MATLAB programming environment which will give better results.

Before applying the interpolation techniques for the experiment, it is necessary to determine the loads applied at the given location. To estimate the values at the load, it is necessary to get the optimum sensor locations, therefore the first step will be to find the

optimum sensor locations. There is a set of procedure that the user has to follow to get the optimum locations and optimum orientation for certain number of strain gages. The procedure is as follows:

1. Generation of the candidate set where gages can potentially be placed.
2. Determination of the number of strain gages to be used, and
3. Determination of D-optimal design that yields optimum location and orientation of strain gages.

3.2 Generation of the Candidate set

The entire structure is meshed into a number of finite elements where the size of the mesh is equal to the size of the strain gage. The locations of the strain gages are not randomly selected. The designer has to follow certain criteria before mounting the strain gage. First, the designer has to eliminate all the inaccessible locations from the entire structure since there will be locations were mounting of strain gage and measuring strain values are going to be impossible. Second, the location where is load is applied should be eliminated. It is sensible to eliminate these locations since the load could damage the strain gage. The remaining locations along with its angular orientation can be considered as the candidate set for optimum sensor placement. In the following section, the procedure to construct $[A]_{candidate}$ matrix will be explained in detail.

The optimum sensor location$[A]^{m\times n}_{optimum}$ is a matrix where m is the number of rows, which represents the number of strain gages required and n is the number of columns which represents the number of locations at which the load will be applied. The structure used for practical purpose is always a 3D model and meshing a 3D model will give 3D elements. But the strain gages mounted on the structure will be on the surface. Hence we need strain values on the surface. One of the best methods to solve this problem is by coating shell elements on the 3D model and measuring the strain values on the surface.

The strain data will measured on the selected elements instead of nodes. The nodal strain data is the average of the adjacent elements strain data. Hence to avoid the averaging, its better to utilize the entire strain data of the element. The strain gage will be located at the centroid of the element. Moreover using nodal strain data will make the strain gage orientation even more complex. Keeping all the reasons in mind, it is recommended to use elemental strain data instead of nodal strain data.

For a load estimation problem, the load is applied at certain locations. Hence, it is very much necessary to select location where the load will be applied. At same location a unit load is applied and the strain tensors are recorded all using a finite element software. The strain tensors at candidate locations are recorded. The value of the strain tensor changes depending on the angular orientation of the strain gage. With the help of the rotation matrices, it is possible to rotate the strain tensor from one coordinate to another, thus giving the results of the strain tensor with a different orientation. Equation(3.4) shows the transformation of the strain tensors from *xyz* coordinate to *x'y'z'*:

$$[\varepsilon]_{x'y'z'} = [T][\varepsilon]_{xyz}][T]^T \tag{3.4}$$

where [T] is the transformation or rotation matrix,which contains the direction cosines for the *x'y'z'* coordinate system with respect to *xyz* coordinate system. For this problem, the rotation are assumed to occur about local z-axis of the element. The transformation matrix is given as follows:

$$[T] = \begin{bmatrix} \cos\theta & \sin\theta & 0 \\ -\sin\theta & \cos\theta & 0 \\ 0 & 0 & 1 \end{bmatrix} \tag{3.5}$$

Each element has 18 different directions at which the strain gages can be placed, and the angle orientation will be from 0 to 170 degree with an increment of 10 degree. The

candidate set will consist of only the strain components acting in the *x'x'* direction since the strain gages are sensitive in the axial direction. Finally, each column of the $[A]_{candidate}$ matrix will consist of the locations of the strain gages and strain data at all candidate locations in all 18 directions.

3.3 Determination of Number of Strain Gages

The number of strain gages needed for any problem is an important aspect. The more the number of strain gages, the more accurate will be the results for the recovered load. Since the strain gages are expensive, this procedure will not be cost-effective. Hence it is necessary to know the required number of strain gages. For the recovery of load, left-pseudo inverse method is used as shown in equation(3.2), therefore it is sensible to state that the number of strain gages should be greater or equal to the number of loads to be estimated.

3.4 Determination of the D-optimal Design

This section explains the procedure followed to identify optimum gage locations which is identification of a set of gage locations along with their angular orientations. After selecting the number of gages g that will be used, an algorithm as shown in Fig(3.1) helps select optimum gages from $[A]_{candidate}$ which will satisfy the conditions discussed in the previous section. It is possible to use the trial and error method but its going to be tedious and time consuming and will not give correct solution. In this case let [A]$\subset R^{g\times m}$ be a random set of g strain gages which is a subset of $[A]_{candidate}$.

Few statisticians, *Mitchell (1974)*, *Galil (1980) and Johnson et al (1983)* have done research and the improved the algorithm which could reduce the variance of the sensitivity of matrix [A]. An appropriate method was used to find $[A]_{optimum}$ which is a set of optimum number of gages and their angular orientation which will maximize the value for determinant of $[A]^T[A]$. The design which maximizes the determinant $[A]^T[A]$ is called

the D-Optimal design. *Mitchell (1974)* presented a D-optimal design where D denotes the determinant of the matrix. D-optimal designs will give low variance among parameters and low correlation between parameters. The main difficulty is the existing local maxima, which can be solved by an efficient algorithm.

The main objective of constructing the D-optimal design is to reduce or to add points to the potential design by using the candidate set of points spaced over the area of interest. *Galil (1980)* and *Johson et al (1983)* generated a new algorithm with D-optimal which included sequential exchange algorithm and k-exchange algorithm respectively. The objectives of this newly built algorithm is very well illustrated in the following paragraph.

The main objective of the algorithm is to calculate a set of of gages that can give least variance, which is to have maximum prediction variance of g rows in $[A]_{optimum}$ matrix. To get a maximum value for g rows, it is necessary to do the augmentation and reduction of *[A]* matrix. With this optimum augmentation, the candidate set with maximum prediction variance value is added as a row to the matrix *[A]*. In the same way, the reduction of the augmented design is achieved by eliminating the candidate gage of matrix with minimum value of prediction variance. This whole procedure of adding and eliminating of candidate points keeps going on in a sequential pattern until and unless no further improvement can be made in the objective function.

The sequential exchange algorithm is explained in detail. The first step is to construct a matrix *[A]*, this matrix consists of number of strain gages g which are randomly selected and represent the row of the matrix and the applied loads m represents the columns. If the candidate matrix consists of n candidate points, then the remaining *(n-g)* are still considered to be the candidate set. Now from the remaining *(n-g)* gages in the candidate set, a candidate point is selected and the corresponding row is augmented to matrix *[A]* to form $[A]_+$ so that a maximum value of determinant of ${[A]_+}^T[A]_+$ can be obtained. After this, the next step is elimination. Out of the $g+1$ rows in matrix $[A]_+$, a row is deleted to construct a matrix $[A]_-$ so that maximum determinant of ${[A]_-}^T[A]_-$ can

be obtained. This process of eliminating and adding of rows continues till no further improvement can be made in the answer for the determinant of $[A]_-{}^T[A]_-$. This procedure should give the least variance for g gages in the $[A]_{optimum}$ matrix. The drawback of this procedure is that it is very expensive to compute the determinant at each step by using $M = \left|[A]^T[A]\right|$. An alternate formula *Gupta,(2013)* for computing the determinant $\left|[A]_+{}^T[A]_+\right|$ from $\left|M\right|$ when the row y^T is augmented to the matrix [A] is:

$$\left|M_+\right| = \left|M\right|(1[+]y^T M^{-1} y) \tag{3.6}$$

where [+] denotes the addition of row which is replaced by subtraction in the case of deleting a row y^T from $[A]_+$. In order to use the equation (3.6), M^{-1} can be maintained and updated as the row y^T is augmented to the matrix [A] by:

$$\left|M_+\right|^{-1} = \left|M\right|^{-1}[-]\frac{(M^{-1}y)(M^{-1}y)^T}{(1[+]y^T M^{-1}y)} \tag{3.7}$$

where [-] denotes subtraction and is replaced by addition in the case of deleting a row y^T from $[A]_+$.

This method of adding and deleting rows continue until the determinant cannot be improved any further. Now the optimum strain gage locations and orientations, $[A]_{optimum}$ are obtained, the strain gages are placed at these optimum locations before the unknown loads are applied. Strain data are measured at these optimum locations, $[\varepsilon(t)]_{optimum}$,when the unknown load is applied to the structure. This forms the strain tensor for unknown load and by using equation(3.8), the unknown load can be estimated.

$$[F(t)]_{estimate} = ([A]^T_{optimum}[A]_{optimum})^{-1}[A]_{optimum}{}^T[\varepsilon(t)]_{optimum} \tag{3.8}$$

This sequential algorithm is described in a flowchart shown in Fig (3.1). This entire algorithm was implemented in MATLAB programming software. The finite element model

of the system was constructed in ANSYS 17.2.

3.5 Numerical Examples

The load recovery technique which is explained from sections 3.1 to 3.4 is illustrated using two examples. The first example is of quasi-static load recovery on a simply supported 3D cantilever beam. The second example is of impact load recovery on a 2D square plate which is clamped at all four corners.

3.5.1 Quasi-Static Load Recovery

Using the concepts from Sec 3.1, a bent cantilever beam is modeled in ANSYS and is subjected to three loads at its tip. The loads will be recovered for quasi-static case in 3 directions, x, y and z directions. A similar experiment will then be used to recover impact load.

Quasi-static loads are like static loads. In static load, the load is calculated for that instant but in case of quasi-static load, it is calculated at each time-step. The load values will be different at each time-step, hence the responses needs to be treated differently. The main objective of doing this experiment is to identify the optimum strain gage locations based on the measured strain data. With the help of the strain data and gage location it will be possible to recover the quasi-static loads.

For this numerical experiment, ANSYS-APDL 17.2 was used. The software is used to model a bent cantilever beam and later the strain data was extracted. The material properties are discussed in Table 3.1.

The thickness is kept constant throughout the entire length which is 0.25 m and the length is 2 m, the height of the beam is kept as 1 m. The beam is isotropic in nature, the dimensions of the beam is shown in Fig (3.2). The entire structure is meshed with SOLID45 elements where each element has eight nodes. After meshing the total number of elements are 600 and nodes are 918. The cantilever beam with elements is shown in

Fig(3.3) and the nodes is shown in Fig(3.4). As discussed in Sec 3.2, the strain is only measured on the surfaces. Therefore to recover surface strains, the best choice is to use the shell coating method. In this case since the thickness of the beam is not very high, it safe to do the experiment without shell coating.

In this example, the location of the load is already known. The load is applied on node 382, this is load to be recovered. The load is applied in three different directions, which are, x, y and z directions. As explained in Sec 3.2, a unit load is applied in all three directions, one at a time, and the strain data is extracted after the load is applied. The strain tensors were calculated for each element for each load case separately. The same logic will be applied for impact load since the impact load acts at one location for a short time.

The strain tensor are transformed using equation(3.5) with angular orientation from 0 to 170 degree with an increment of 10 degree, which forms a candidate set. According to Sec 3.3 the number of strain gages should be more than the loads to be estimated. In this problem, the number of loads applied are three hence the number of strain gages used are four. The algorithm from Sec 3.4 was used to find the optimum strain gage location and angular orientations. The gage location and angular orientation is showed in Fig(3.5) and the listed in Table 3.2 . After the optimum location is identified, quasi-static loads were applied at the same time on node 382. The loads are applied in different directions as follows:

1. Sine wave of amplitude 1.0 and frequency 2.0 in x direction.

2. Random load in the range [0,1] in y direction.

3. Square wave of amplitude 3.0 and frequency 2.0 in z direction.

The strain data is obtained only at the optimum location. The strain tensors are recovered at each time step, the load is applied as a separate static analysis. The results of the applied and recovered load is shown from Fig(3.6) to Fig(3.8).

3.5.2 Impact Load Recovery

In this example, the impact load is recovered at a particular node of the 2D metal plate. The entire illustration is shown in Fig(3.9). The material used for the square plate is steel which has Young's Modulus E = 200GPa and Poisson's ratio is equal to 0.3. The length of each side is 3.0 m. The plate is meshed with SOLID182 elements,and in total it has 25 elements. and 36 nodes. Any one of the degree of freedom is constrained for corner nodes 1, 2, 7 and 12. For node 1 the x-dof is constrained, node 2 the y-dof is constrained , node 7 the x-dof is constrained and node 12 the y-dof is constrained. The complete illustration is shown in Fig (3.10).

It is very difficult to decide the location or the node where the load will be applied since the impact could occur anywhere on the plate. Hence for this experiment a unit load was applied at all nodes except nodes 1, 2, 7 and 12, where the degree of freedoms are constrained. After the unit load application, the strain data were obtained, which was used to find the optimum locations for the placing the sensors. After scanning the entire plate where the load could be applied at a particular node, the set of optimum location were identified. The details are illustrated in the Table (3.3). In this experiment it is assumed that the load is applied at node 9.

By using equation (3.5), the strain tensors at different directions was estimated at each gage location. In this case, two loads are taken into consideration hence the number of load cases nlc is 2. the number of gages used should be more than 2 hence g = 5. The D-optimality criterion, as discussed earlier, is used to find the optimum gage locations and angular orientations for the number of strain gages to form $[A]_{optimum}$. The optimum gage locations and orientations are listed in table, and the elements corresponding to the optimum gage locations are depicted in Fig(3.11).

The same method is followed for reconstruction of impact loading like quasi static load in the earlier example. In this example, the load is only applied for a short span of time and the strain data is obtained. Two load cases are taken into consideration:

1. Half sine wave of amplitude 1.0 acting for 0.2 sec in x direction

2. Square wave of amplitude 3.0 acting for 0.2 sec in y direction.

The load here is only applied from 0.0 sec to 0.2 sec. There is no load applied for the remaining 0.21 to 1.01 seconds. Since the optimum location was already obtained, the strain data is obtained at the optimum location. To recover the load, equation(3.8) is used and load can be recovered for time steps from 0.0 to 1.0 sec. The graphs for applied and recovered loads are given in Fig(3.12) to Fig(3.13).

Table 3.1: Properties of a Bent Cantilever Beam

Material Property	Value(*SI units*)
Young's Modulus	200 GPa
Poison's ratio	0.3
Density	$7635 kg/m^3$

Table 3.2: Optimum Gage Location and Orientation for a Bent Cantilever Beam

Gage Number	Optimum Gage Location(Element Number)	Orientation(Degrees)
1	39	0
2	237	20
3	162	0
4	161	0
5	23	0

Table 3.3: Properties of a Steel Plate

Material Property	Value(*SI units*)
Young's Modulus	200 GPa
Poison's ratio	0.3
Density	$7635 kg/m^3$

Table 3.4: Optimum Gage Location and Orientation for a Steel Plate After Applying Load at node 8

Gage Number	Optimum Gage Location(Element Number)	Orientation(Degrees)
1	5	100
2	10	10
3	25	10
4	20	60
5	15	110

Table 3.5: Optimum Gage Location and Orientation for a Steel Plate After Applying Load at node 9

Gage Number	Optimum Gage Location(Element Number)	Orientation(Degrees)
1	10	10
2	15	100
3	25	110
4	20	60
5	5	110

Table 3.6: Optimum Gage Location and Orientation for a Steel Plate After Applying Load at node 10

Gage Number	Optimum Gage Location(Element Number)	Orientation(Degrees)
1	25	60
2	20	100
3	15	10
4	5	110
5	10	10

Table 3.7: Optimum Gage Location and Orientation for a Steel Plate After Applying Load at node 11

Gage Number	Optimum Gage Location(Element Number)	Orientation(Degrees)
1	25	60
2	20	100
3	5	110
4	15	10
5	10	10

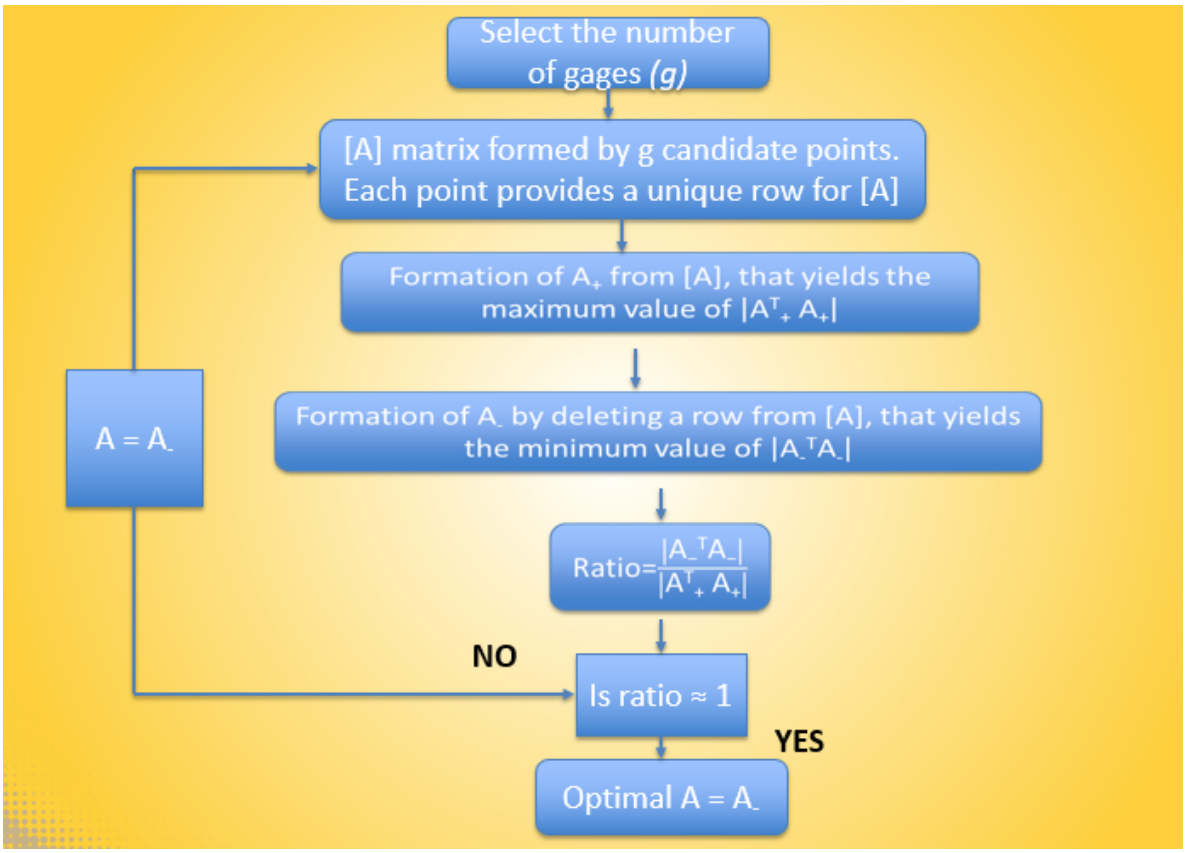

Figure 3.1: Flowchart of the Sequential Exchange Algorithm

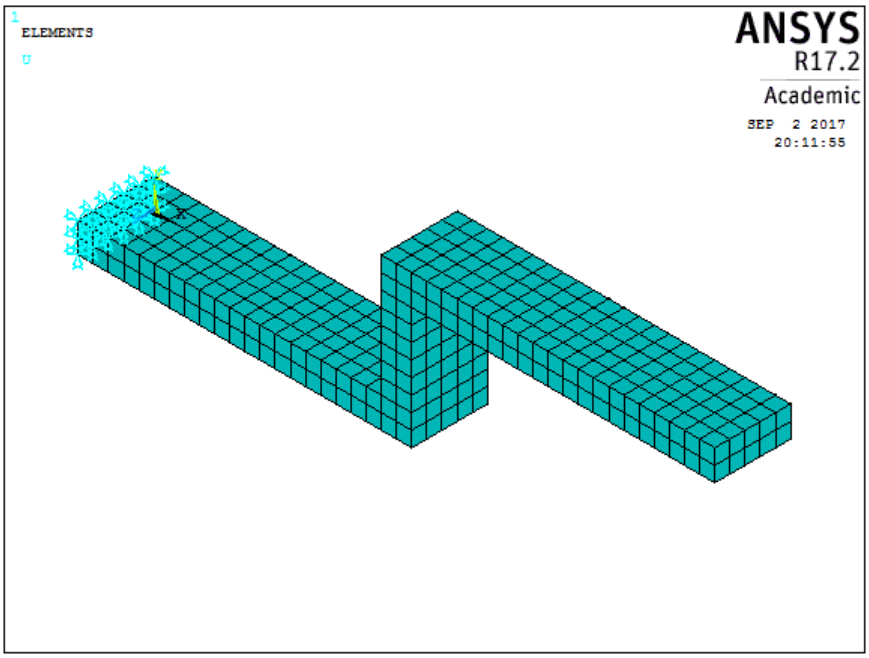

Figure 3.2: Simply Supported 3D Cantilever Beam

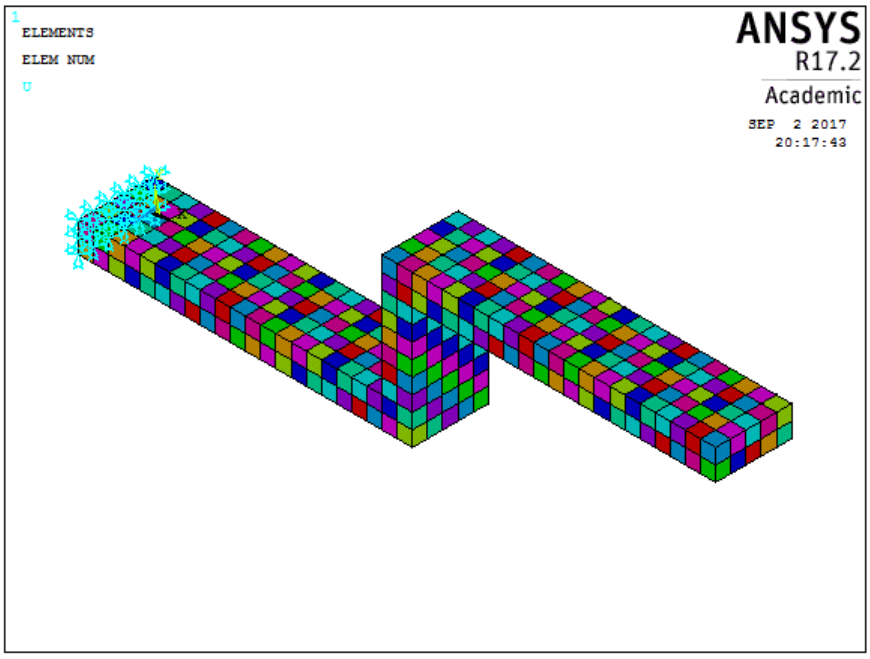

Figure 3.3: Solid Elements of a Cantilever Beam

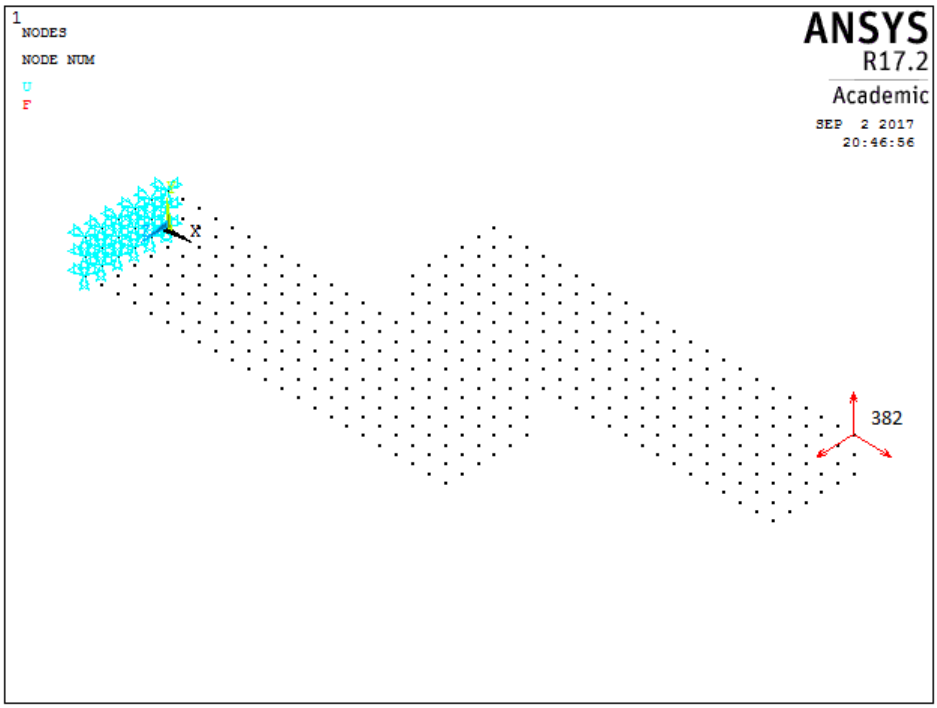

Figure 3.4: Loads Applied at node 382

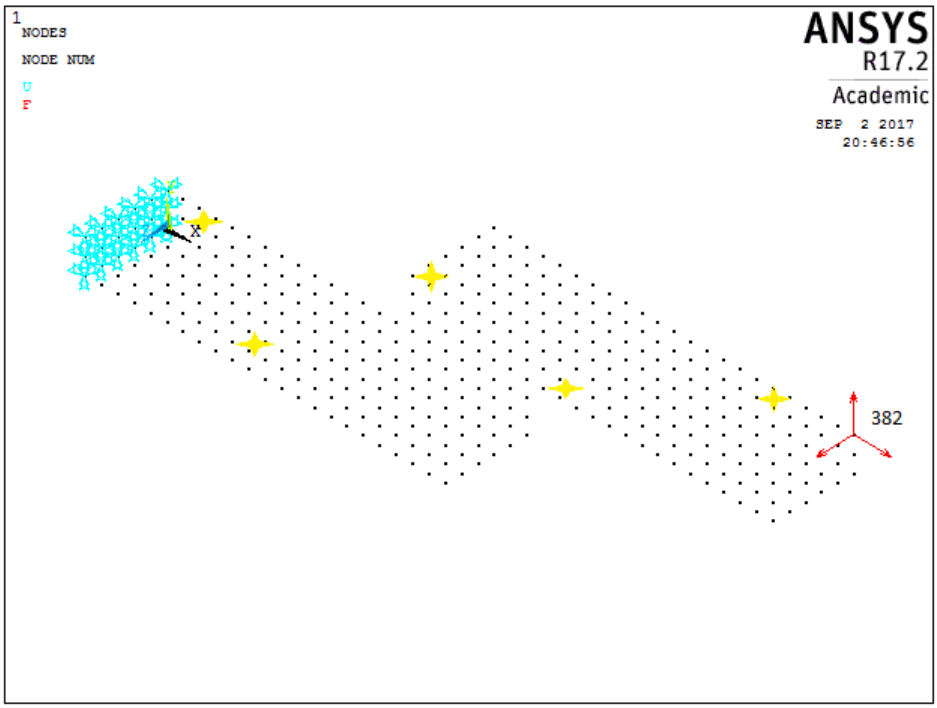

Figure 3.5: Optimum Gage Locations

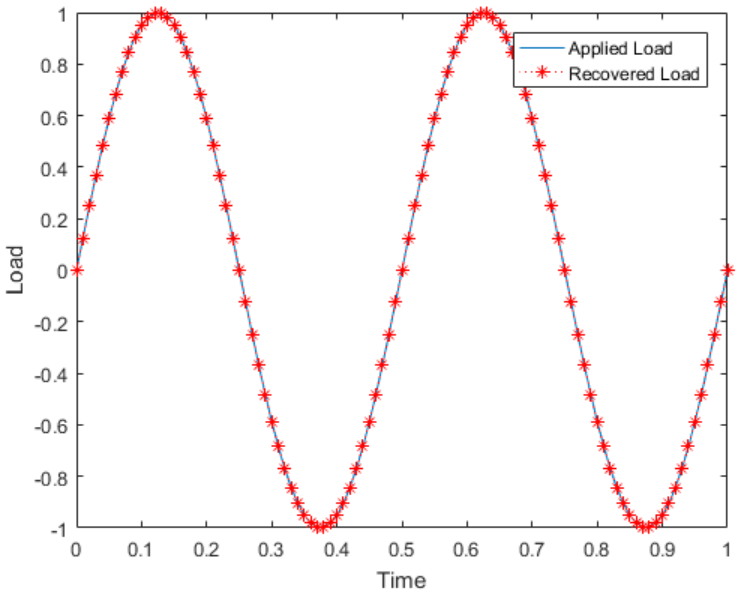

Figure 3.6: Recovery of Sine Wave Load

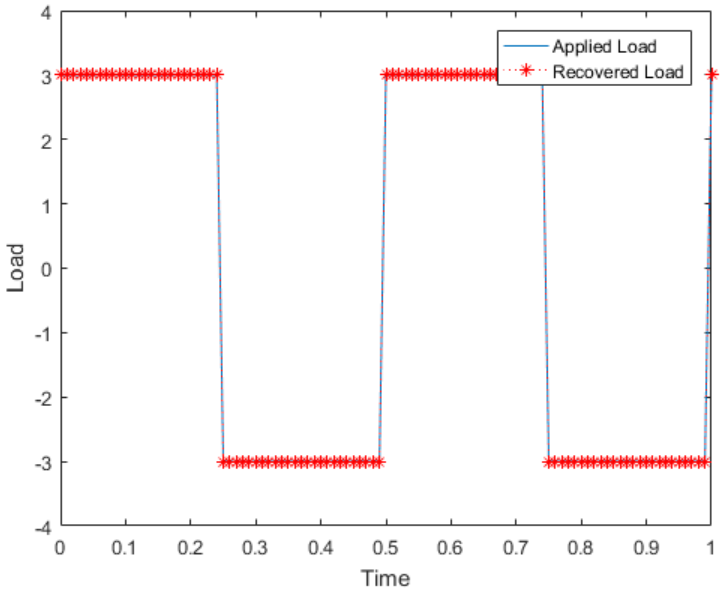

Figure 3.7: Recovery of Square Wave Load

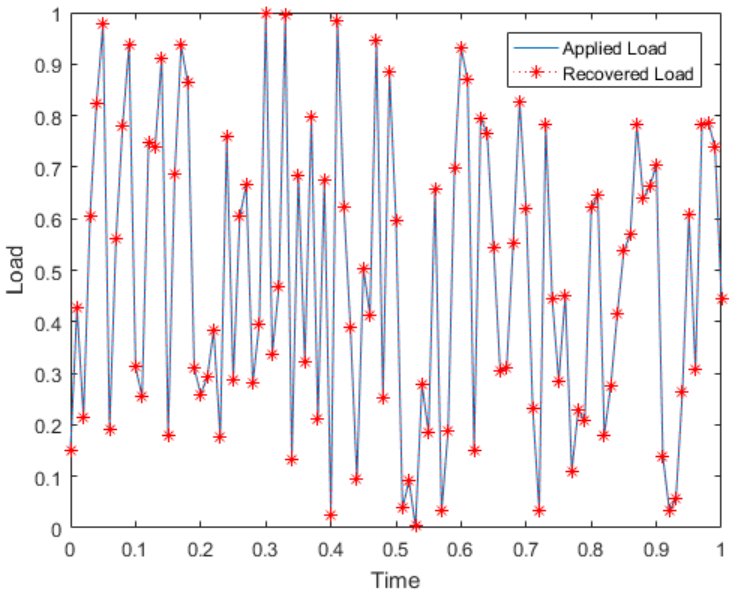

Figure 3.8: Recovery of Random Wave Load

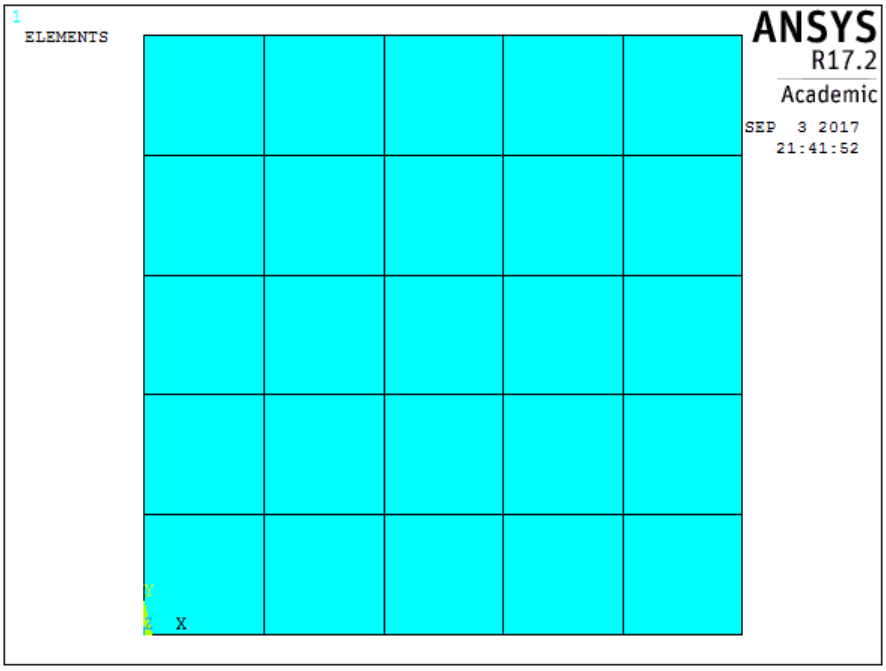

Figure 3.9: 2D Steel Plate Constrained on All Four Corners

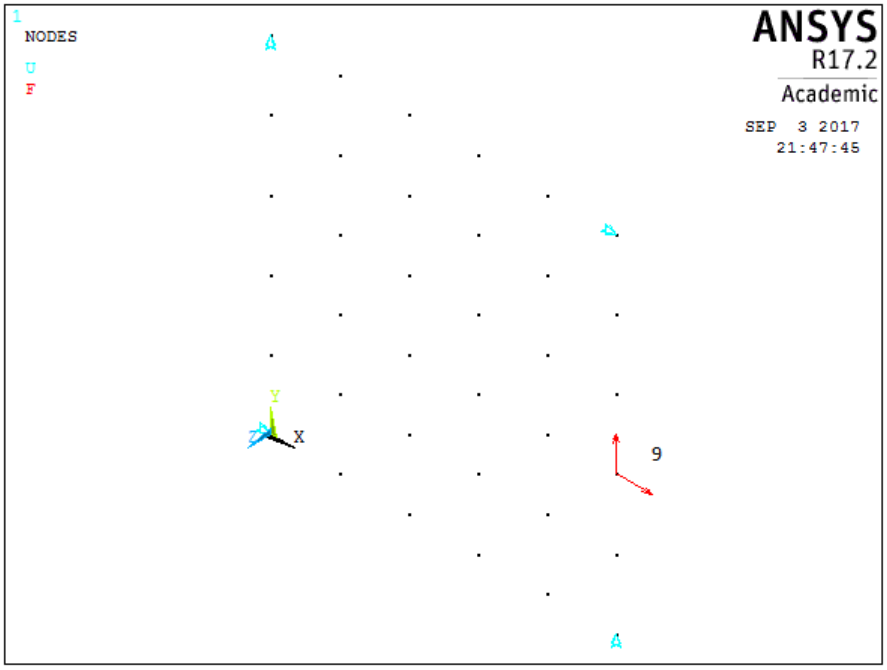

Figure 3.10: Impact Load applied on Node 9 along x-axis and y-axis

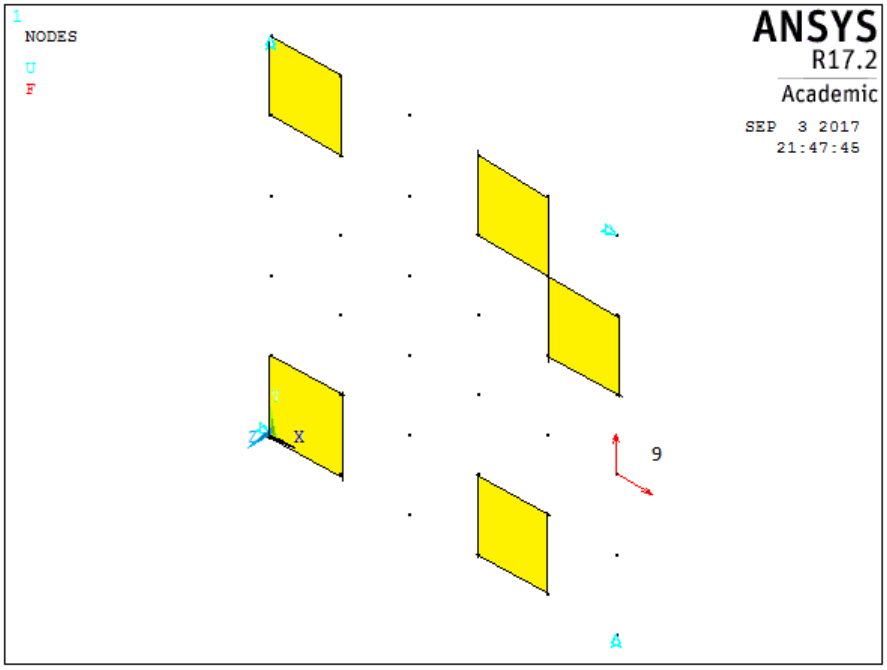

Figure 3.11: Optimum Gage Locations

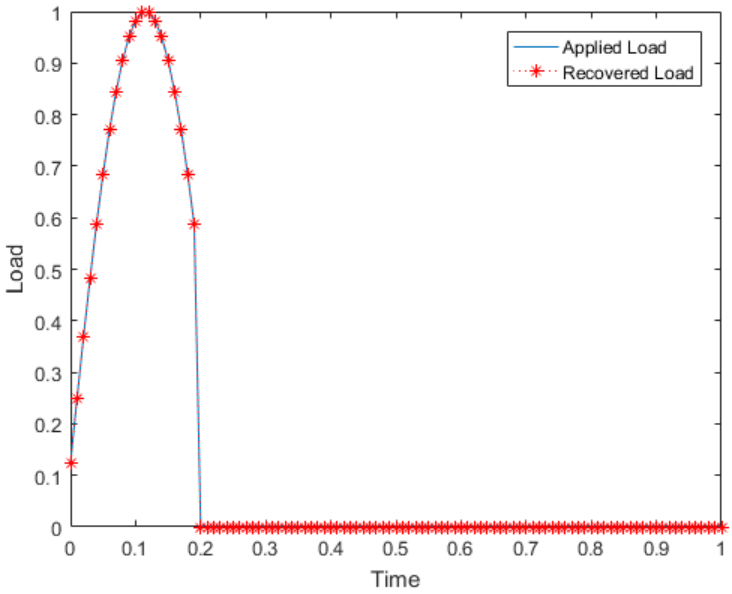

Figure 3.12: Recovery Of Impact Sine Wave Load

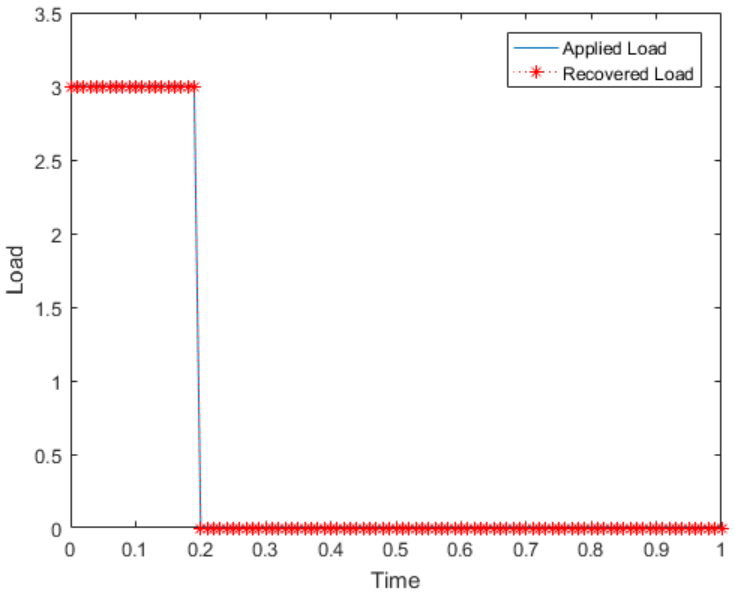

Figure 3.13: Recovery Of Impact Square Wave Load

4 Impact Load Recovery Using Model Reduction and Strain Gages

This chapter deals with the recovery of dynamic impact load using the information about mass, stiffness matrices and acceleration and displacements. The theories and equations used to obtain the recovered load are discussed in Secs 4.1 and Secs 4.2. There is an assumption made throughout the chapter that the structure which is used for the problem is linear in nature.

4.1 Matrix Representation of Structural Dynamics of a System

The response of structure can be represented in many different ways such as use of Partial differential equations, ordinary differential equations, discrete mass and stiffness matrices, finite element method etc.

4.1.1 Physical Coordinate Representation

A simple structure subjected to external loads can be represented using partial differential equation. But as the problem complexity increases, it becomes difficult to calculate the response of the structure using partial differential equations. In such situations, finite element analysis will be the best approach. In finite element analysis, the structure is divided into small elements. The size and the shape of the mesh can be defined by the user.

For a system represented by linear second order differential equations, the response to the load, is represented as follows:

$$F(t) = [M]\ddot{x}(t) + [C]\dot{x}(t) + [K]x(t) \tag{4.1}$$

where $[M]$ and $[C]$ $[K]$ are the mass, damping and the stiffness matrices of the structure

respectively. This entire system can be modeled using finite element analysis software. The displacement x(t) is the structural displacement vector and Force F(t) is the structural force vector.

4.1.2 Modal Coordinate Representation

For a complex system, it is very tedious to calculate the value for $[M]$, $[C]$ and $[K]$, at such times it is easier to extract these matrices from finite element model. The availability of the system response which is the displacement x(t) of the system will help in estimation of the dynamic load F(t). In the later part of the chapter, it is shown that the system response of the structure can be calculated by Modal analysis. Once the displacement is obtained, $\dot{x}(t)$ and $\ddot{x}(t)$ can be calculated using numerical differentiation techniques. With the availability of x(t), $\dot{x}(t)$ and $\ddot{x}(t)$ the dynamic load can be calculated. The value of x(t) can be obtained by assuming a harmonic solution

$$x(t) = Asin(wt) \tag{4.2}$$

where A= vector of constants ω =natural frequency t is time in seconds An eigenvalue problem is calculated to solve modal analysis problem. The equation for eigenvalue and eigen vector is shown below

$$([w^2][M] - [K][\phi])[\phi] = [0] \tag{4.3}$$

which gives the mode shapes and natural frequencies. The displacement can be calculated by using the mode shape and mode participation factor at each degree of freedom.

$$x(t) = q_1(t)[\phi]_1 + q_2(t)[\phi]_2 + ... + q_n(t)[\phi]_n \tag{4.4}$$

$$[x(t)]_{n\times t} = [\phi]_{n\times n}[q(t)]_{n\times t} \tag{4.5}$$

where n is the total degrees of freedom and q(t) is the mode participation factor. The modes have to be normalized with respect to mass matrix to decouple the modal coordinates of the system. The normalized matrices [K] and [M] are given in equation(4.6) and equation(4.7) below.

$$[\phi]^T[M][\phi] = [I] \tag{4.6}$$

$$[\phi]^T[K][\phi] = [\omega^2] \tag{4.7}$$

Here, [I] is the identity matrix and the diagonal matrix $[\omega^2]$ contains system eigenvalues (square of natural frequencies)

$$[w^2] = \begin{bmatrix} w_1^2 & 0... & 0 \\ 0 & w_2^2... & 0 \\ . & . & . \\ 0 & 0 & w_n^2 \end{bmatrix} \tag{4.8}$$

Equation (4.1) can be modified using the mode participation factor q(t) and mode shapes and can be expressed as:

$$F(t) = [M][\phi][\ddot{q}(t)] + [C][\phi][\dot{q}(t)] + [K][\phi][q(t)] \tag{4.9}$$

4.2 Model Order Reduction

Model order reduction methods, also known as condensation methods, target reducing the degrees of freedom of a model without changing substantially the dynamic properties of the system. In this thesis, the model order reduction techniques have been used extensively. These techniques are applied in the research and explained below.

4.2.1 Static Condensation (Guyan Reduction)

Static condensation technique also known as Guyan reduction technique which was developed by *Guyan (1965)* is the most basic technique of reduction. The dynamic properties are ignored in this technique, hence the name Static condensation. This technique has been used very often and is described below. The moment of inertia and damping effects are neglected for the structure and the equation (4.1) is rewritten as follows:

$$[K]x(t) = F(t) \tag{4.10}$$

In the above equation, all degrees of freedom are taken into consideration. But while performing the condensation techniques, some degree of freedom are retained while others are ignored. These degrees of freedom are divided into two groups :

(a) Master degrees of Freedom

(b) Slave degrees of freedom

The master degrees of freedom will be the one where the external force is applied and the rest would be the slave degrees of freedom. The degrees of freedom are categorized in such manner because the slave degree of freedom will not have much information. After dividing the degree of freedom as master or slave degrees of freedom, the equation is rearranged as

follows:

$$\begin{bmatrix} K_{mm} & K_{ms} \\ K_{sm} & K_{ss} \end{bmatrix} \begin{bmatrix} x_m(t) \\ x_s(t) \end{bmatrix} = \begin{bmatrix} F_m(t) \\ F_s(t) \end{bmatrix} \tag{4.11}$$

The superscripts 'm' and 's' are the master and slave degrees of freedom. Since the slave degrees of freedom does not have any external force applied, the equation can be expressed as follows:

$$[K_{sm}]x_m(t) + [K_{ss}]x_s(t) = F_s(t) = 0 \tag{4.12}$$

The main purpose of static reduction is to reduce a full system into a reduced model. The displacement of the structure with the master and slave degrees of freedom can be expressed as follows:

$$x(t) = \begin{bmatrix} x_m(t) \\ x_s(t) \end{bmatrix} = \begin{bmatrix} I_{mm} \\ -K_{ss}^{-1}K_{sm} \end{bmatrix} x_m(t) \tag{4.13}$$

where I is the identity matrix which conforms to the dimension of master degrees of freedom. The transformation matrix is given as $[T_{guyan}]$ and expressed as follows:

$$[T_{guyan}] = \begin{bmatrix} I_{mm} \\ -K_{ss}^{-1}K_{sm} \end{bmatrix} \tag{4.14}$$

The mass, stiffness and force matrix is reduced by using the transformation matrix as shown in equation(4.15) and equation(4.17). The equation is expressed as follows:

$$[M_{reduced}] = [T_{guyan}^T][M_{guyan}][T_{guyan} \tag{4.15}$$

$$[K_{reduced}] = [T^T_{guyan}][K_{guyan}][T_{guyan} \tag{4.16}$$

$$[F_{reduced}] = [T^T_{guyan}][F_{full}] \tag{4.17}$$

Equations(4.15)-(4.17) form the static reduction.

4.2.2 Component Mode Synthesis

Component Mode Synthesis, also known as CMS, was proposed by *Craig and Bampton (1968)*, hence also known as the Craig-Bampton reduction method. This technique basically involves substructuring of the model. The degrees of freedom are divided into two sets:

(a) Boundary degrees of freedom (b)

(b) Internal degrees of freedom (i)

The boundary degrees of freedom are those which are common to two or more substructures, where as the internal degrees of freedom are the one which are relevant to a particular substructure. Ignoring the damping condition, the model is substructured into matrix form. The matrix equation is expressed as follows:

$$\begin{bmatrix} M_{bb} & M_{bi} \\ M_{ib} & K_{ii} \end{bmatrix} \begin{bmatrix} \ddot{x}(t)_b \\ \ddot{x}(t)_i \end{bmatrix} + \begin{bmatrix} K_{bb} & K_{bi} \\ K_{ib} & K_{ii} \end{bmatrix} \begin{bmatrix} x(t)_b \\ x(t)_i \end{bmatrix} = \begin{bmatrix} F(t)_b \\ F(t)_i \end{bmatrix} \tag{4.18}$$

where $x(t)_b$ is the displacement at boundary degrees of freedom and $x(t)_i$ is the displacement at internal degrees of freedom. Since the internal degrees of freedom will have near zero external force acting on it and considering the stiffness matrix alone, the second part of the same gives the following equation:

$$x(t)^s_i = -[K]^{-1}_{ii}[K]_{ib}x(t)_b \tag{4.19}$$

The sum of the static modes and normal modes is equal to the displacement of the internal degrees of freedom. The equation(4.20) below forms the solution for eigenvalue problem, which forms the constrained modal matrix $[\phi]_c$ and constrained normal modes, $x(t)_i^n$ are expressed in equation(4.21)

$$-[w^2][M]_{ii} + [K]_{ii} = 0 \tag{4.20}$$

$$x(t)_i^n = [\phi]_c q(t)_p \tag{4.21}$$

where p is the number of constrained modes. The constrained modes are generally less than the internal degrees of freedom. The displacement vector are given by:

$$x(t) = \begin{bmatrix} x(t)_b \\ x(t)_i \end{bmatrix} = \begin{bmatrix} x(t)_b \\ -[K]_{bb}^{-1}[K]_{ib}x(t)_b + [\phi]_c q(t)_p \end{bmatrix} \tag{4.22}$$

$$= [\psi]_{CB} \begin{bmatrix} x(t)_b \\ q(t)_p \end{bmatrix} \tag{4.23}$$

$[\psi]_{CB}$ is the transformation matrix. This transformation matrix transforms the full model into a reduced model. The transformation matrix is expressed as follows:

$$[\psi]_{CB} = \begin{bmatrix} [I] & [0] \\ -[K]_{ii}^{-1}[K]_{ib} & [\phi]_c \end{bmatrix} \tag{4.24}$$

The reduced CB mass, stiffness and damping matrices are expressed as follows:

$$[M]_{CB} = [\psi]_{CB}^T [M]_{full} [\psi]_{CB} \tag{4.25}$$

$$[K]_{CB} = [\psi]_{CB}^{T}[K]_{full}[\psi]_{CB} \tag{4.26}$$

$$[C]_{CB} = [\psi]_{CB}^{T}[C]_{full}[\psi]_{CB} \tag{4.27}$$

$$x(t)_i^s = -[K]_{ii}^{-1}[K]_{ib}x(t)_b \tag{4.28}$$

It is seen that Guyan reduction model works for small eigenvalues, but given high frequencies, this method gives inaccurate results. The CB method retains dynamic information and has been shown to give better results than static condensation techniques.

4.2.3 Modal Analysis and Strain Modes

The displacement at any point x(t) is directly related to the strain data of the structure by a linear differential operator D:

$$\varepsilon(t) = Dx(t) \tag{4.29}$$

$$\varepsilon(t) = [\psi^{\varepsilon}]q(t) \tag{4.30}$$

where $[\psi^{\varepsilon}]$ is the modal strain data. Equation(4.30) expresses the strain data as a linear combination of strain modes and mode participation factors. The normal modes and strain modes are an intrinsic property of a structure. Generally in real world application, all the mode details are available but only reduced number of modes m are taken into consideration, which leads to truncated $[\psi^{\varepsilon}]$ which contains the details of the retained modes m

$$[\varepsilon(t)] = [\psi^{\varepsilon}][q(t)]_m \tag{4.31}$$

where $[q(t)]_m$ is the mode participation factor for the retained modes. $[\psi^{\varepsilon}]$ is already known, since the details are obtained from finite element method, $[\varepsilon(t)]$ is measured and by least square method q(t) can be calculated by the following equation:

$$q(t) = ([\psi^{\varepsilon}]^T[\psi^{\varepsilon}])^{-1}[\psi^{\varepsilon}]^T[\varepsilon(t)] \tag{4.32}$$

There are few limitation that has been encountered while calculating q(t):

1. The strain data $[\varepsilon(t)]$ is only available at optimum location. It is not possible to measure the strain data at all location, since it is not feasible to place the strain gages at all location. Hence $[\varepsilon(t)]$ cannot be obtained for full structure.

2. The strain gages cannot be mounted on or around the input force location.

3. The potential location for strain gages can be large number, but only few location should be selected since a lot of strain gages cannot be used. It is very much necessary to which location would be feasible and how many number of strain gages can be used.

4.2.4 Candidate set

The number of strain gages, *(g)* used are based on the number of retained modes, *(m)* i.e g > m. The candidate set is generated by using the finite element model of the structure. A modal analysis is performed on the structure. The number of retained modes can be the total number of degrees of freedom, but only certain number of modes can be taken into consideration. The decision is made depending on the MPF of the retained modes which is recovered after the load is applied on the structure. The modal mass at the modes are captured by the retained number of modes, which can be used to decide the number of modes that can be retained for the analysis. It is observed than the more the number of retained modes, the better would be the results. The modal matrix $[\phi]$, [M],[C] and [K] can be extracted from finite element model.

Next, each retained mode is applied one at a time as a displacement load on the structure. Strain data are obtained at each retained node which is expressed in equation(4.31). The number of shell elements suitable for mounting strain gages be c; the strain tensors are obtained at each element for each load case. The angle orientation keeps changing at the gages, hence the strain tensors are transformed like shown in section 3.2. The transformed strain tensors provide the candidate set $[\psi]_{cs}$

4.2.5 D-optimal Design

It is not possible to extract the strain data at all possible location, therefore to obtain approximate solution a candidate set $[\psi]_{cs}$ needs to be identified. In terms of a randomly selected subset $\tilde{\psi^{\varepsilon}}$, the approximate solution for equation (4.32) can be expressed as follows:

$$q\tilde{(t)} = ([\tilde{\psi^{\varepsilon}}]^T[\tilde{\psi^{\varepsilon}}])^{-1}[\tilde{\psi^{\varepsilon}}]^T[\varepsilon\tilde{(t)}] \tag{4.33}$$

where $q\tilde{(t)}$ is the approximation vector and $[\tilde{\varepsilon}]$ is the strain vector at randomly chosen locations on the structure. It can be noted that $\tilde{\psi^{\varepsilon}}$ plays an important role for the recovery of dynamic load like [A] does in quasi static load. Since $q\tilde{(t)}$ is obtained from from inverse problem techniques which are usually ill conditioned, the accuracy of q(t) depends on the number of strain gages, location of strain gages and angular orientations. Using the D-optimal design algorithm as mentioned in section(3.4), the candidate set is found so that the $[\psi]_{opt}$ can be determined. Once, $[\psi]_{opt}$ is known strain gage location and angular orientation are determined, the time dependent strain data $[\varepsilon(t)]_{opt}$ is measured. The strain value $[\varepsilon(t)]_{opt}$ is replaced in above equation, and the equation is expressed as follows:

$$q\tilde{(t)} = ([\psi^{\varepsilon}]^T_{opt}[\psi^{\varepsilon}]_{opt})^{-1}[\psi^{\varepsilon}]^T_{opt}[\varepsilon(t)]_{opt} \tag{4.34}$$

Next using q(t), and mode shape $[\phi]$ the displacement x(t) can be determined. By numerically differentiating the displacement, the velocity $\dot{x}(t)$ and acceleration $\ddot{x}(t)$ can be obtained. The [M], [C] and [K] can be determined by the finite element model using all the details the force F(t) can be obtained. The theory is explained using numerical examples in the next section.

4.3 Error Quantification

The percentage of error can be calculated between the applied and recovered loads. The root mean square (RMS) error $\varepsilon\%$ is given as:

$$\varepsilon\%_{error} = (\frac{\sqrt{(Fa - Fr)}^2}{\sqrt{Fa^2}})X100 \tag{4.35}$$

where Fa is the applied load and Fr is the recovered load.

4.4 Dynamic load estimation on a cantilever beam

The dynamic load is estimated using a cantilever beam example. In this case, a sinusoidal load is acting at one end of the cantilever beam needs to be estimated. Here a finite element model of a cantilever beam is developed in ANSYS using SOLID45 elements. The top and bottom surface of the cantilever beam is considered since these are the potential location for strain gages, hence these surfaces are meshed with SHELL41 elements. The modulus of elasticity, thickness and density of the shell element are given near zero values. All the degrees of freedom are constrained at the left end of the cantilever beam. The model of the cantilever beam is shown in Fig(4.1). The model consist of 160 elements, 200 unconstrained nodes and each node has 3-degrees of freedom. The beam in total has 600 degrees of freedom.

A sinusoidal load is applied at the free end of the cantilever beam. The main intention is to obtain the optimum location for strain gages. The relevant input data like

the gage location angle orientation are illustrated in Table(4.1).

There are few things that need to be completed to calculate the dynamic load. A modal analysis is performed on the beam where only 7 transverse modes were extracted. The torsional modes where ignored in this case. These transverse modes formed the modal matrix $[\phi]$. By using finite element method, [M] and [K] matrix were obtained in a Harwell-Boeing format. Since the Harwell-Boeing format cannot be used for calculations, hence with the help of MATLAB programming, the [M] and [K] matrices were assembled of the first 17 modes that were retained, each mode is applied as a displacement load on the beam, one at a time and strain data was obtained. Ignoring the ten torsional and out of plane bending modes, the number of retained modes were 7. The strain data of these 7 modes were obtained from ANSYS. Since the retained modes were 7, the number of gages used should be more than the retained modes, for this example 9 gages were taken into consideration. Using D-optimality criterion optimum strain data, the gage location and angular orientation are obtained. The gage locations on the cantilever beam are shown in Fig(4.2).

A transient load is applied at one end of the cantilever beam. Since this is a time dependent load, the strain data was obtained at each time step for each element. The mode participation factor for 7 retained modes at each time steps were recorded. The MPF was recovered using equation (4.34). The exact MPF obtained from ANSYS were compared with the recovered MPF. The plots are shown from Fig(4.3) to Fig(4.5). Next the displacement x(t) was calculated using equation(4.21) and with numerical differentiation the velocity $\dot{x}(t)$ and acceleration $\ddot{x}(t)$ were obtained. The applied load f(t) was finally calculated using equation (4.9).The graph of the applied load and recovered load is shown in Fig(4.6).

As shown in Fig (4.6), the recovered load is not as same as the applied load. This approach seems to be straight forward but it suffers from some limitations. The total number of modes for the cantilever beam are 600 out of which only 7 modes were used to

calculate the load, which causes a large truncation error. The higher the number modes of retained modes, the better will be results for recovered load. The results will be better than Fig(4.6), but still far off from the applied load.

The best results could be obtained only unless all modes are retained. All 600 modes used for the analysis, in that case where the number of strain gages should also be at least 600. This procedure would be less cost effective and practical as there will be constraints, where to place the strain gages. To overcome this limitation, model order reduction approach was proposed. This approach results in significant improvement in the results. The Model Order Reduction is explained in the next section.

4.4.1 Dynamic load estimation using Model Order Reduction Technique

The cantilevered beam is now modeled using the Craig Bampton method. The input data is tabulated in Table(4.2). After the transient load is applied, the displacement data are obtained which is differentiated numerically to find the velocity and acceleration. Equation (4.22) is used to assemble the displacement vector. The CB model was run with different number of modes were taken into consideration. The recovered force was calculated for 5, 7 10 and 15 retained modes were calculated. The results are shown in Fig (4.7), Fig (4.8), Fig (4.9) and Fig (4.10). As shown, the load estimation results are better for more modes. Equation (4.35) is used for Error quantification and the results are shown in Table (4.3).

Table 4.1: Input Data for a Cantilevered Beam

Variable	Value	Variable	Value
n	600	c	160
m	7	g	8

Table 4.2: Input Data for a Cantilevered Beam with CB reduction

Variable	Value	Variable	Value	Variable	Value
n	600	c	160	g	8
m	7	b	395,425,469,486	p	3

Table 4.3: Error Quantification based on number of modes used

Number of Retained modes	RMS error %
5	2.5401 %
7	1.4048 %
10	1.3086 %
15	1.2579 %

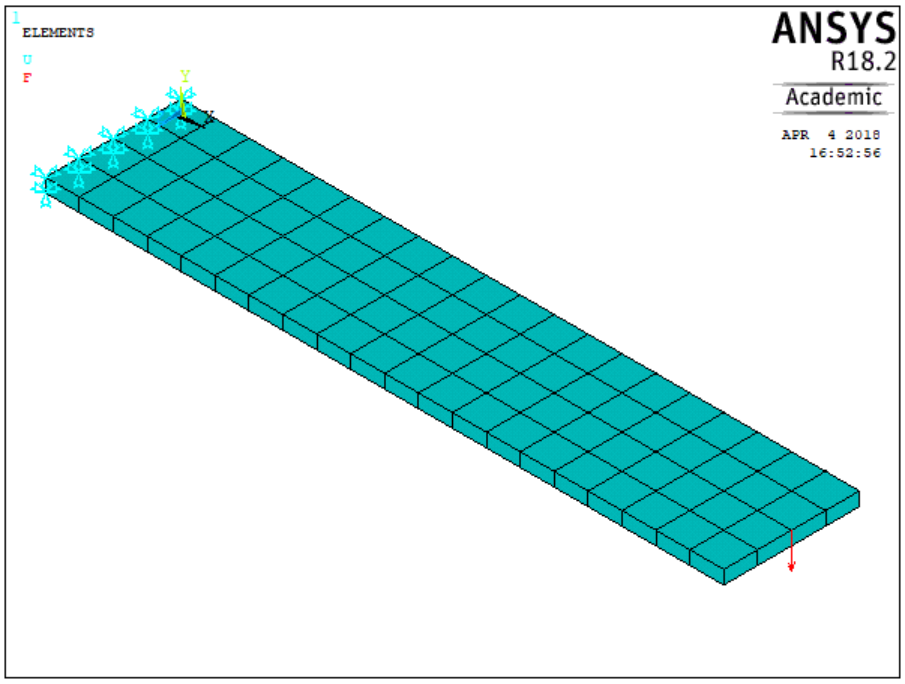

Figure 4.1: Finite element model of Cantilever beam with applied load

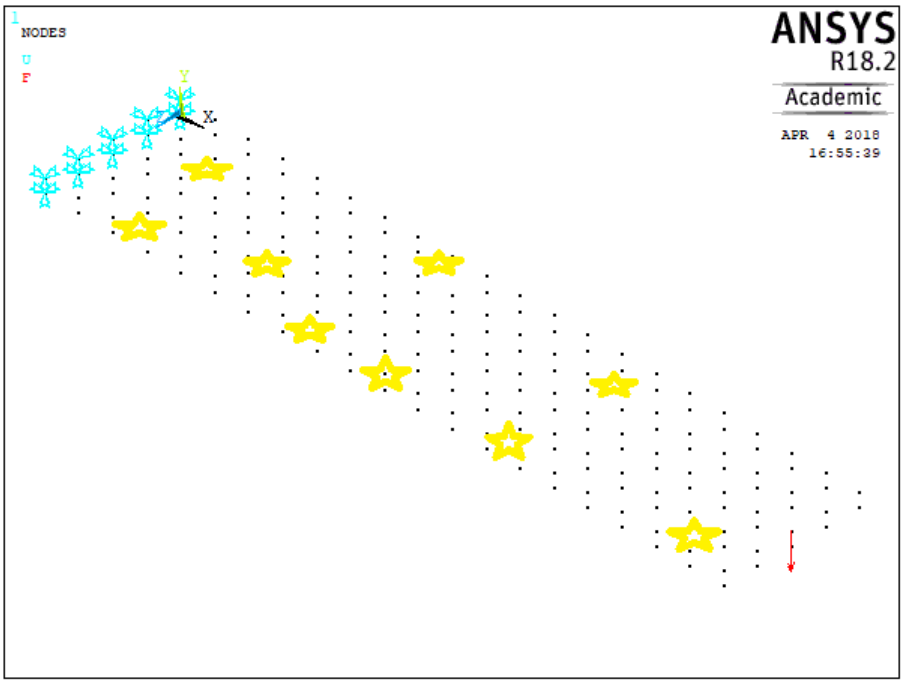

Figure 4.2: Optimum location for strain gages

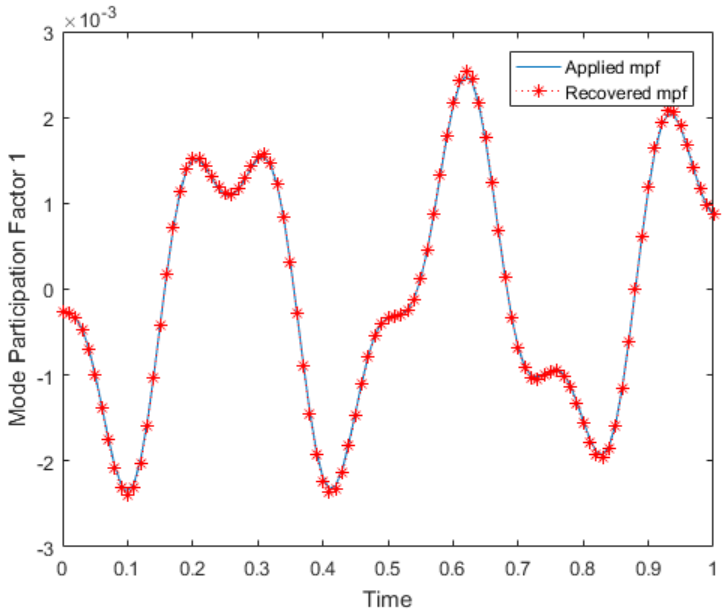

Figure 4.3: Participation factor for 1st retained mode

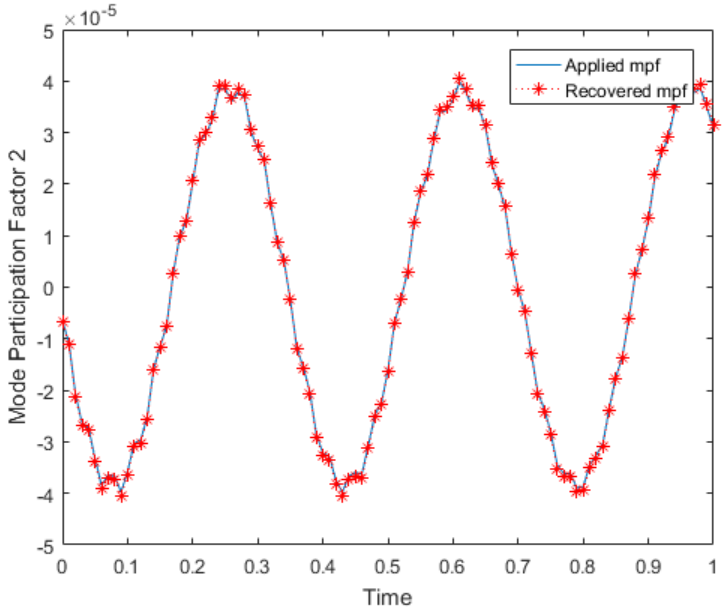

Figure 4.4: Participation factor for 2nd retained mode

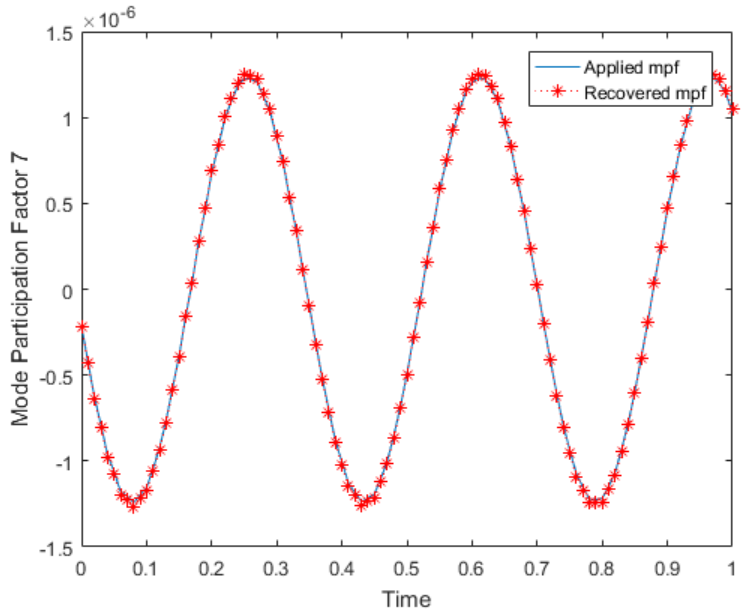

Figure 4.5: Participation factor for 7th retained mode

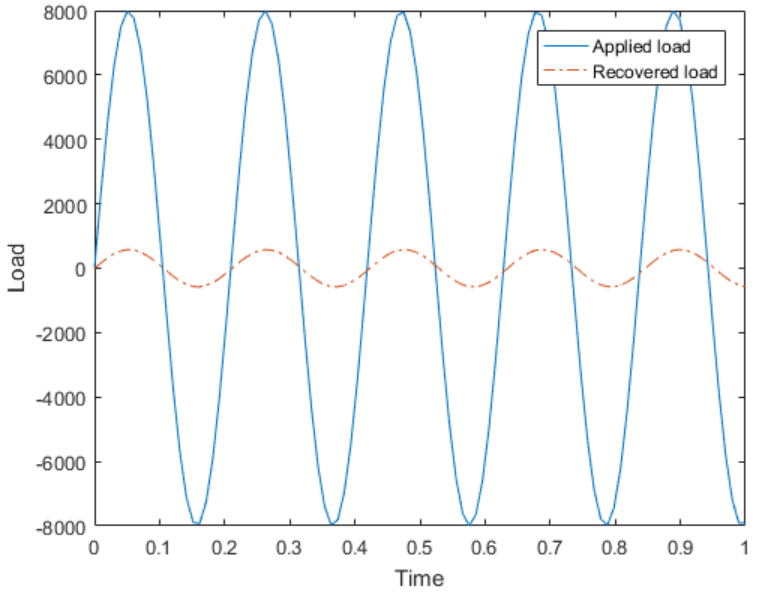

Figure 4.6: Recovered Load with 7 retained modes without Reduction

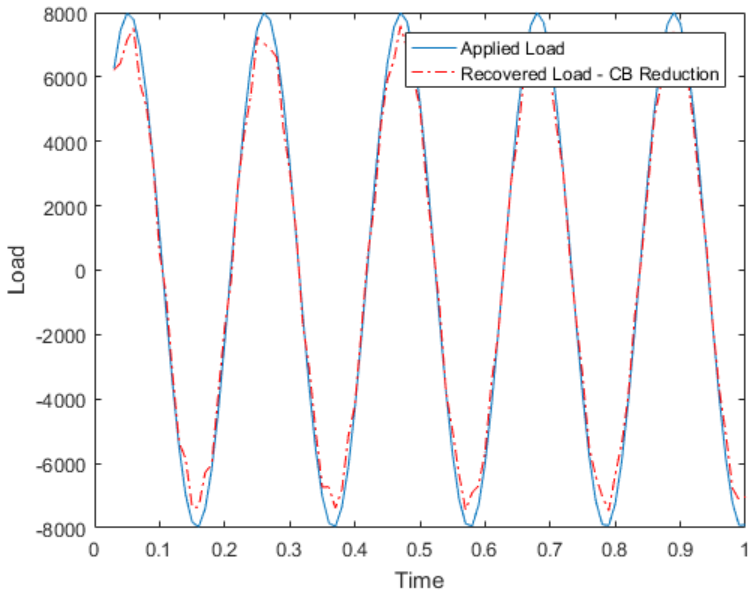

Figure 4.7: Recovered Load with 5 retained modes with CB Reduction

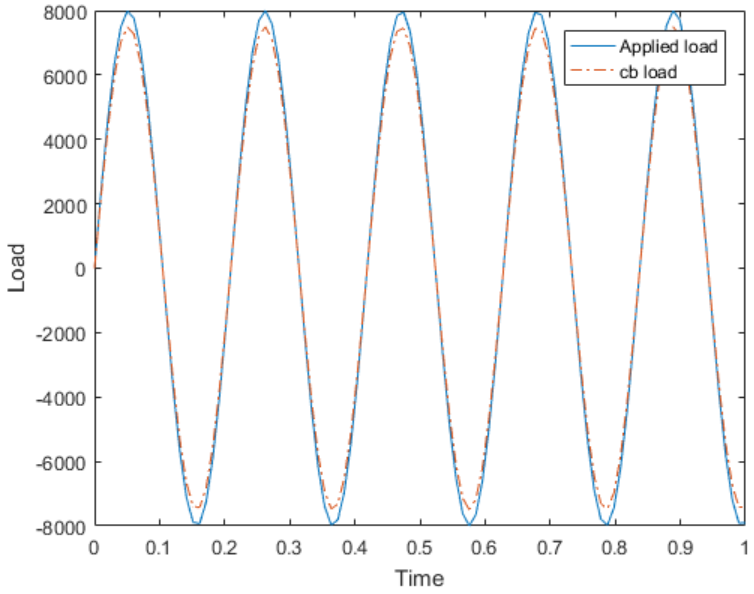

Figure 4.8: Recovered Load with 7 retained modes with CB Reduction

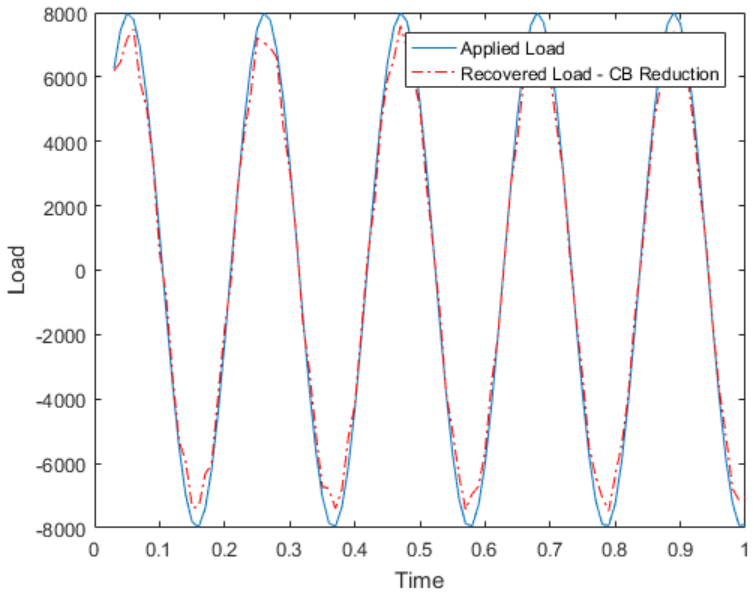

Figure 4.9: Recovered Load with 10 retained modes with CB Reduction

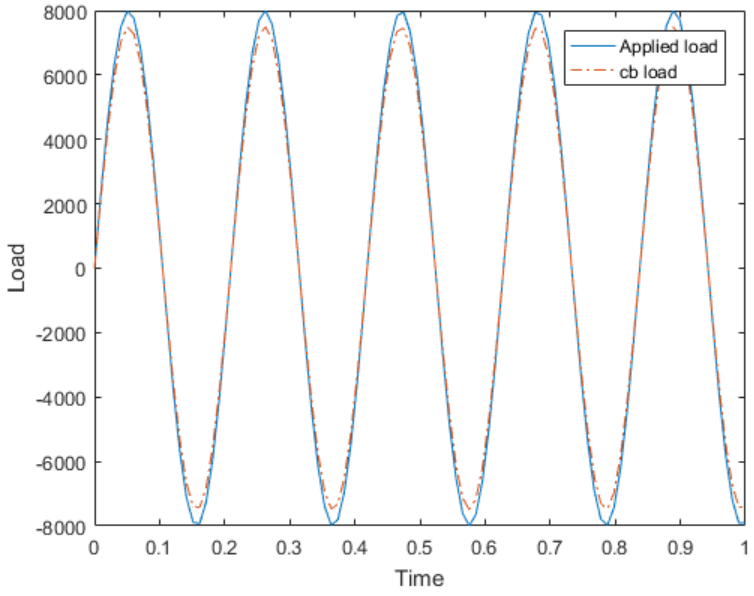

Figure 4.10: Recovered Load with 15 retained modes with CB Reduction

4.5 Impact Load recovery Using D-optimal Design and Craig-Bampton Model Reduction

Next, a square plate structure was used to recover impact load. Here three different types of impact loads are recovered sine load, triangular pulse and a square load.

4.5.1 Square plate with internal damping condition

The cantilever beam example used in the above section had some limitations. Since the beam has one end free, there are few torsional modes recorded. These modes were discarded, since they were not relevant to motion under consideration. For the cantilever as explained in the earlier section, out of 17 retained modes only 7 modes could be used for the analysis. In this section, the Craig - Bampton Model reduction technique was applied on a square plate which is constrained on all four sides. Since the plate is constrained along all four edges there won't be any torsional modes recorded. A finite element model of the square plate was modeled in ANSYS. The model has 648 d.o.f and each node has 3 degrees of freedom. The square plate model is shown in Fig(4.11). In this section proportional Rayleigh damping is used to model material damping. Rayleigh damping is applied to the model using constants $[\alpha]$ and $[\beta]$ given by following equation:

$$\alpha + \beta\omega_i^2 = 2\omega_i\zeta_i \tag{4.36}$$

where $[\omega]$ is the natural frequency. Here $[\omega]$ value is taken as 1750 HZ, $[\zeta]$ is 0.01 and $[\alpha]$ is assigned as zero. Substituting the values the calculated value for $[\beta]$ is obtained as:

$$\beta = 0.000014 \tag{4.37}$$

The load data is recovered at each time step the impact load is applied to the square plate. With these values, the displacement, velocity and acceleration can be calculated. The

procedure followed is same as the one followed for cantilever beam. The modal analysis is performed and five modes were retained for load reconstruction. The input data is tabulated in Table(4.4) and Table(4.5). Since there are no torsional modes for this structure, all the 5 retained modes can be used which form the $[\psi]$ matrix. The shell elements corresponding to optimum strain gage/locations are shown in Fig(4.12). Now an impact load is applied at the center of the plate which is node [250]. The CB model reduction technique is used to recover the applied load. The results for 5 modes are shown in Fig (4.13), Fig (4.14) and Fig (4.15) respectively. The results obtained when 7 modes, 10 modes and 15 modes are retained are also analyzed. Using RMS error quantification, the error percentage by varying number of retained modes is tabulated in Table(4.6). The same methodology is used to recover triangular and square load. It is seen from Table 4.6 that as the number of retained modes increases, the RMS error between applied and recovered load reduces.

Table 4.4: Input Data for a Square plate

Variable	Value	Variable	Value
n	648	c	260
m	5	g	6

Table 4.5: Input Data for a Square plate with CB reduction

Variable	Value	Variable	Value	Variable	Value
n	648	c	260	g	6
m	5	b	16,250,259,284	p	3

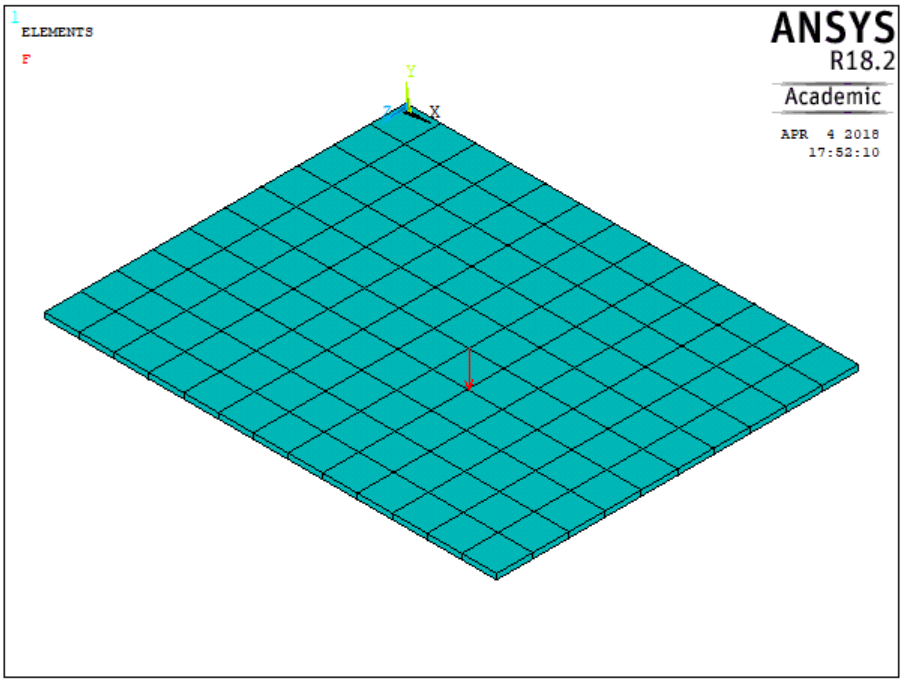

Figure 4.11: Aluminum plate with applied load

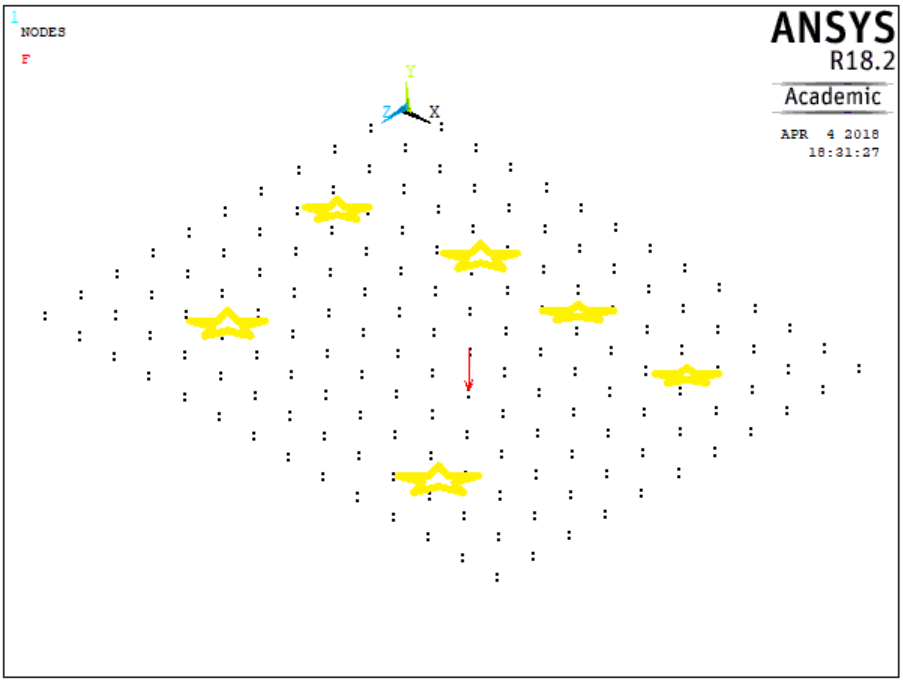

Figure 4.12: Optimum Gage Locations

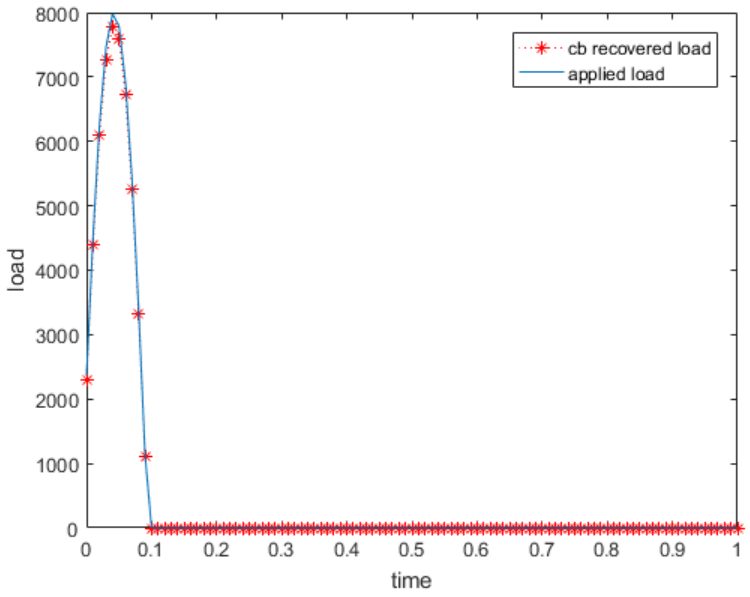

Figure 4.13: Recovery of Half Sine Impact Load

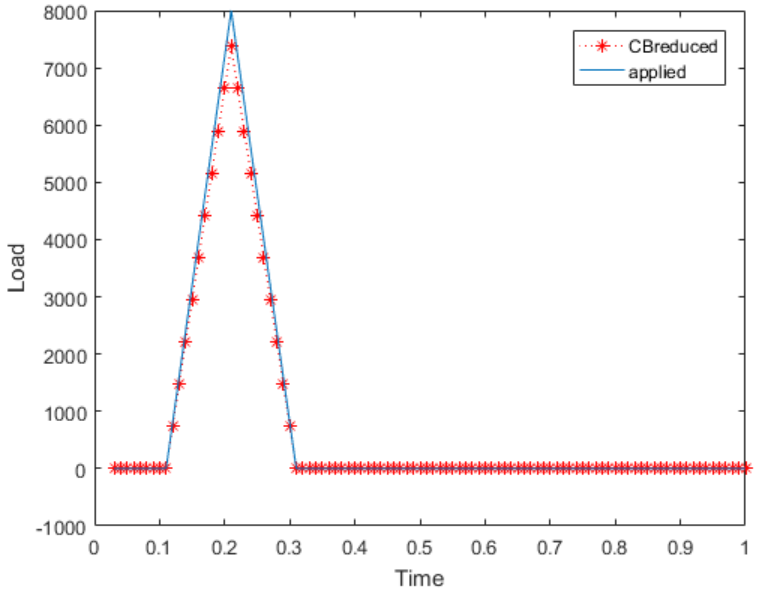

Figure 4.14: Recovery of Triangular Pulse

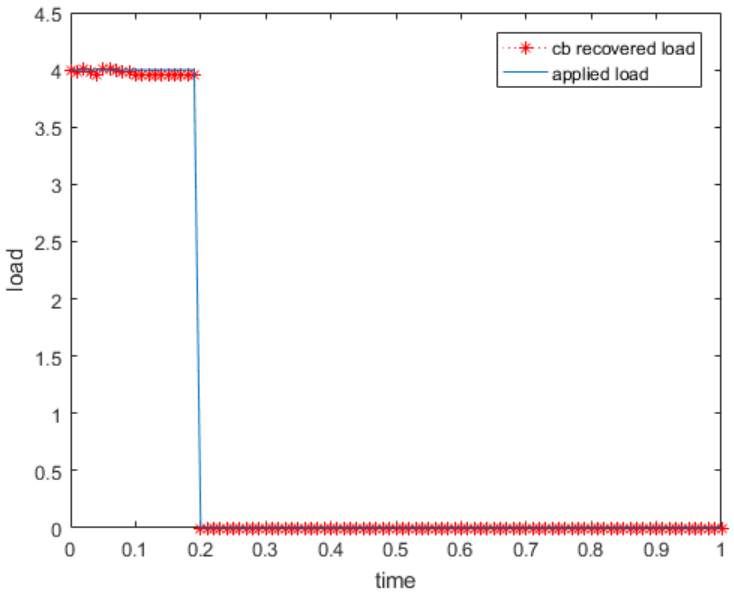

Figure 4.15: Recovery of Square Pulse

Table 4.6: Error Quantification based on number of modes

Number of retained modes	RMS error %
5	2.377 %
7	2.126 %
10	1.893 %
15	1.371 %

4.6 Summary

In this chapter computational techniques are presented to recover the applied load using strain measurement at optimum gage locations. It has been observed that by increasing the number of retained modes, the load recovery results turn out to be more accurate and as shown in results, the RMS error also reduces. But its not always feasible to extract large number of modes, since that would increase the number of strain gages which will eventually make the entire procedure less cost-effective. The best approach to overcome this limitation would be to reduce the size. Hence Model reduction techniques were proposed. It has been observed the Craig-Bampton reduction technique gives very good results, but there are few limitation to it. The selection of suitable boundary condition, is really important for this technique. Only when appropriate boundary conditions are chosen, the method yields accurate results.

5 Summary

In this thesis, different algorithms were discussed to recover quasi-static, transient as well as impact loads using optimum placement of sensors. Chapter 1 explained the problem statement and the importance of the thesis in detail. For an optimized design, it is important to identify the true value loads imposed on the system. In past direct methods, such as placing load cells at specific location have been used. This method had a lot of limitation. These limitations are solved by the indirect method. Here the structure itself is considered as a transducer which can be called a "self transducer". The most important factor in solving the inverse problem is the sensor location. The optimum sensor locations and orientations are selected based on the algorithm presented in chapter 3. If the optimum locations are not chosen wisely, the locations where the structural response is recorded will not give accurate estimate of the applied load. Hence to avoid ill-conditioning of estimated recovered load, it is very much necessary that the optimum location of sensors be used.

Chapter 2 presents the literature review where an optimum sensor location can be used to recover imposed load. In Chapter 3, the concept of D-optimal design is explained in detail. With the D-optimal algorithm it is possible to recover quasi-static, transient as well as impact loads. The main concept of D-optimal is to find the optimum strain gage locations and optimum strain gage orientations. The strain data is only measured at these locations. As the point of load application changes, the optimum sensor locations can change. Through a simple example presented in chapter 3, the influence of load location on sensor placement is examined. It was seen that certain sensor locations are always selected irrespective of point of load application. The results presented show that accurate load estimates are obtained even when point of actual load application is not known a priori.

Chapter 4 deals with the recovery of transient as well as impact loads using strain modes of the structure. The system response was reconstructed using strain and displacement modes. To reduce the problem size, model order reduction technique are used. The model reduction technique used here is Craig-Bampton method. The accuracy of the load estimation is better when the number of modes are increased, which are shown in section(4.4). For the proposed procedure to be used, the number of strain gages should be more than the number of modes retained in analysis. Increasing the number of modes will not always be feasible as it will lead to an increasing number of sensors. This problem is solved by using model reduction techniques where limited number of modes are used. The results obtained using CB reduction yielded accurate results. Once again D-optimal algorithm is used for optimum placement of sensors.

6 Conclusions and Future Work

The main goal of this thesis was to use inverse technique to estimate impact load using strain data. As shown in chapter 3 and chapter 4 it is possible to estimate impulse load using this technique. It is seen that as the number of retained modes increases, the quality of load estimates becomes better. However this improvement comes at the expense of an increase in number of sensors. To reduce the number of sensors needed, model order reduction techniques are also explored. Two reduction techniques namely Guyan and Craig-Bampton reduction were tried. It is observed that the quality of load estimates using Craig-Bampton technique are better and the computational time to solve the problem also reduces. In this technique, as the number of retained modes increases the load estimates improved.

For the CB model reduction technique, an optimum set of boundary degrees of freedom are needed. Since the structure used in this thesis are simple, hence the boundary degree of freedom were easy to select. But in case of complicated structures it will become difficult to select the optimum boundary degree of freedom. An automated procedure should be explored where the optimum boundary degrees of freedom can be established. This will enhance the usability of the algorithm developed for strain gages.

The analysis done in this thesis was purely computational, it should be possible to estimate load experimentally too. This is left as an area of future work. Further it would be interesting to explore if the inverse techniques can be used to recover the impact load for non-linear materials past the yield point.

7 References

1. Zareian F. Simplified Performance-Based Earthquake Engineering Ph.D. dissertation Department of Civil and Environmental Engineering, Stanford University, Stanford, California, 2006.

2. Caughey, T.K., O Kelly, M.E.J. Classical Normal Modes in Damped Linear Dynamic Systems Transactions of ASME, Journal of Applied Mechanics 32 (1965) 583-588.

3. Rayleigh, L. Theory of Sound (two volumes), 1954th ed., Dover Publications, New York, 1877

4. L. F. Ibarra, R. A. Medina and H. Krawinkler, Hysteretic Models that Incorporate Strength and Stiffness Deterioration, Earthquake Engineering and Structural Dynamics, Vol. 34, No. 12, 2005, pp. 1489-1511.

5. A. Alipour and F. Zareian, Study Rayleigh Damping in Structures; Uncertainties and Treatments, in 14 th World Conference on Earthquake Engineering: Innovation Practice Safety, 2008.

6. B. Hillary and D. J. Ewins, The use of strain gauges in force determination and frequency response function measurements, in Proceedings of the 2nd International Modal Analysis Conference (IMAC '84), pp. 627634, Orlando, Fla, USA, 1984.

7. ANSYS Mechanical APDL Element Reference, Release 15.0, Help System,Structural Analysis Guide, ANSYS, Inc.

8. Desanghere G., 1983, Identification of External Forces based on Transferfunction Measurements: Frequency Response Method, Proceedings of the 8th Int. Seminar on Modal Analysis, Kath. Univ., Leuven, Belgium, pp. 1-28.

9. Medina R.A., Krawinkler H. Seismic demands for non-deteriorating frame structures and their dependence on ground motions PEER Report 2003/15. Berkeley (CA):

Pacific Earthquake Engineering Research Center; 2004.

10. S.Y. Khoo and Z.Ismail (2013) Impact force identification with pseudo-inverse method on a lightweight structure for under-determined, even-determined and over-determined cases International Journal of Impact Engineering, page # 52-62

11. Yan G, Zhou (2009) L. Impact load identification of composite structure using genetic algorithms, Journal of Sound and Vibration, page # 3-5

12. Guyan, R. J. (1965). Reduction of Stiffness and Mass Matrices. American Institute of Aeronautics and Astronautics (AIAA) Journal, 3 (2), 380.

13. Gupta, D. (2013). Inverse Methods for Load Identification Augmented by Optimal Sensor Placement and Model Order Reduction. Ph.D Dissertation, University of Wisconsin Milwaukee. U.S.A.

14. Mitchell, T. J. (1974). An Algorithm for the Construction of D-Optimal Experimental Designs. Technometrics, Vol. 16(2), pp.203-210.

15. Galil, Z. (1980). Time-and Space-Saving Computer Methods to Mitchells DETMAX, for Finding D-Optimum Designs, Technometrics, Vol. 22, pp.301-313.

16. Johnson, M., Nachtsheim, C. J. (1983). Some Guide Lines for Constructing Exact D-Optimal Designs on Convex Design Spaces, Technometrics, Vol. 25(3), pp.271-277

17. Craig, R. R., and Bampton, M. C. (1968). Coupling of Substructures for Dynamic Analysis. American Institute of Aeronautics and Astronautics (AIAA) Journal, 6 (7), 1313-1319